Biomass and Bioenergy 81 (2015) 322–338

Contents lists available at ScienceDirect

Biomass and Bioenergy

journal homepage: http://www.elsevier.com/locate/biombioe

Research paper

Differences in the chemical structure of the lignins from sugarcane bagasse and straw

José C. del Río [a, *], Alessandro G. Lino [a, b], Jorge L. Colodette [c], Claudio F. Lima [b], Ana Gutiérrez [a], Ángel T. Martínez [d], Fachuang Lu [e], John Ralph [e], Jorge Rencoret [a]

[a] Instituto de Recursos Naturales y Agrobiología de Sevilla (IRNAS), CSIC, PO Box 1052, E-41080 Seville, Spain
[b] Department of Chemistry, Federal University of Viçosa, Viçosa, MG 36570-000, Brazil
[c] Department of Forestry Engineering, Federal University of Viçosa, Viçosa, MG 36570-000, Brazil
[d] Centro de Investigaciones Biológicas (CIB), CSIC, Ramiro de Maeztu 9, E-28040 Madrid, Spain
[e] Departments of Biochemistry and Biological Systems Engineering, The Wisconsin Bioenergy Institute, and the DOE Great Lakes Bioenergy Research Center, University of Wisconsin, Madison, WI 53726, USA

ARTICLE INFO

Article history:
Received 25 February 2015
Received in revised form
29 June 2015
Accepted 6 July 2015
Available online xxx

Keywords:
Saccharum spp.
NMR
DFRC
Tricin
Lignin acylation
p-Coumarates

ABSTRACT

Two major residues are produced by the sugarcane industry, the fibrous fraction following juice extraction (bagasse), and the harvest residue (straw). The structures of the lignins from these residues were studied by pyrolysis coupled to gas chromatography-mass spectrometry (Py-GC/MS), nuclear magnetic resonance (NMR), and derivatization followed by reductive cleavage (DFRC). Whereas the lignin from bagasse has a syringyl-rich *p*-hydroxyphenyl:guaiacyl:syringyl (H:G:S) molar composition of 2:38:60, the lignin from straw is guaiacyl-rich (H:G:S of 4:68:28). The compositional differences were also reflected in the relative abundances of the different interunit linkages. Bagasse lignin was primarily β–*O*–4′ alkyl-aryl ether substructures (representing 83% of NMR-measurable linkages), followed by minor amounts of β–5′ (phenylcoumarans, 6%) and other condensed substructures. The lignin from straw has lower levels of β-ethers (75%) but higher relative levels of phenylcoumarans (β–5′, 15%) and dibenzodioxocins (5–5/4–*O*–β, 3%), consistent with a lignin enriched in G-units. Both lignins are extensively acylated at the γ-hydroxyl of the lignin side-chain (42% and 36% acylation in bagasse and straw), predominantly with *p*-coumarates (preferentially on S-units) but also with acetates (preferentially on G-units) to a minor extent. Tetrahydrofuran structures diagnostically arising from β–β-coupling (dehydrodimerization) of sinapyl *p*-coumarate or its cross-coupling with sinapyl alcohol were found in both lignins, indicating that sinapyl *p*-coumarate acts as a monomer participating in lignification. The flavone tricin was also found in the lignins from sugarcane, as also occurs in other grasses.

1. Introduction

Sugarcane (*Saccharum* spp. hybrids) is a perennial monocotyledonous plant belonging to the Gramineae (Poaceae) family that has received considerable recent attention due to its potential for biofuel production. The plant originates from Asia but it is well adapted to most tropical and subtropical climates where it has become one of the most important bioenergy crops. Its C4 photosynthesis makes it one of the most efficient species in carbon conversion and one of the most productive amongst all cultivated crops. Sugarcane is the main feedstock for sugar production, accounting for nearly two thirds of the world's production and is also the main raw material for the production of ethanol for automotion [1,2]. World sugarcane production was estimated to be around 1.91 Gt in 2013, about 0.77 Gt produced in Brazil alone, with an average productivity of 75 t ha^{-1} [3].

During the harvest of sugarcane, the leaves and tops are left in field, whereas the stalks are transported to the mill where they are crushed to extract the sugar juice for the production of sugar and ethanol. Two major residues are produced by the sugarcane industry, the fibrous fraction following juice extraction (named bagasse), and the harvest residue (straw). These wastes are produced in large quantities, about 280 million metric tons of bagasse and straw per year [4], and they are expected to increase in the near

* Corresponding author.
E-mail address: delrio@irnase.csic.es (J.C. del Río).

http://dx.doi.org/10.1016/j.biombioe.2015.07.006
0961-9534/

future as this crop expands and new industrial plants are brought online.

The use of lignocellulosic biomass as a feedstock for the production of biofuels and other bio-based products, in the context of the so-called lignocellulosic biorefinery [5], has recently expanded, due in part to concerns about declining fossil fuel reserves, global climate change produced by greenhouse gas emissions from fossil fuels, and the need to secure more localized energy supplies. In this sense, there is an increasing trend towards the more efficient and rational use of agro-industrial wastes, including sugarcane bagasse and straw, as a means to maximize the use of agricultural resources. Sugarcane bagasse and straw are lignocellulosic materials basically composed of cellulose, hemicelluloses, and lignin, with lower amounts of extractives and ash, and are therefore attractive feedstocks for the production of new products, including the production of second-generation bioethanol due to their high carbohydrate contents and their essential independence from competition with food/feed demands [4–9]. Currently, in most of the sugar industries, only the sugar juice is fermented to ethanol, whereas the bagasse and straw are mostly used for generating heat and electricity. The production of second-generation bioethanol from these 'waste' materials could be advantageous for the sugarcane industries as they can capitalize on the infrastructure already in place for the production of first-generation bioethanol. Converting bagasse and straw to ethanol requires an enzymatic saccharification of the polysaccharides to fermentable reducing sugars and their subsequent fermentation to ethanol or other liquid fuels. However, the architecture of the cell-wall, and particularly the presence of the recalcitrant lignin polymer, reduce the accessibility of the enzymes to the cellulose, and decrease the efficiency of the hydrolysis. Costly and harsh pretreatment processes are therefore needed to circumvent cell-wall recalcitrance by removing, or cleaving and redistributing, the lignin polymer [4–13]. Pretreatment is the most important limiting step in the production of ethanol from lignocellulosic materials. The efficiency of the pretreatment process is highly dependent on both the lignin content and structure, and therefore a knowledge of the structure of the lignin polymers in sugarcane bagasse and straw is important to develop appropriate pretreatment methods for delignification, as well as for potentially higher-value utilization of the lignin. However, bagasse and straw residues differ in their physical nature and chemical composition and the required delignification pretreatments will therefore be different for each residue; understanding the composition and structure of the lignins from sugarcane bagasse and straw is paramount.

Lignin is a complex aromatic heteropolymer produced by the combinatorial oxidative coupling of three main monolignols, *p*-coumaryl, coniferyl and sinapyl alcohols, differing in their degrees of methoxylation. When incorporated into the lignin polymer, these monolignols produce differently linked *p*-hydroxyphenyl (H), guaiacyl (G), and syringyl (S) lignin units, respectively, generating a variety of structures within the polymer, including alkyl-β-aryl ethers, phenylcoumarans, resinols, spirodienones and dibenzodioxocins, among others [14]. The lignin composition varies between plants from different taxa and even between different tissues and cell-wall layers from the same plant. Generally, lignin from hardwoods is composed of S and G units in different ratios, whereas lignin from softwoods is composed essentially of G units with minor amounts of H units, and lignins from grasses contain the three units, with H-units still comparatively minor. In addition, the *p*-hydroxycinnamates (*p*-coumarates and ferulates) widely occur in the grass polymers (hemicellulosic polysaccharides and lignin), with *p*-coumarates acylating the γ-OH of the lignin side-chains, and predominantly on S-units, whereas ferulates acylate arabinosyl residues of arabinoxylan chains and participate in both polysaccharide–polysaccharide and lignin-polysaccharide cross-coupling reactions [15].

Despite the large effort devoted to the use of sugarcane bagasse and straw as feedstocks for the production of second-generation bioethanol and other bioproducts [2,4,6–13], the structure of their lignins has not been studied in detail to date, although some studies on the structure of bagasse lignin have been published in recent years [16–18], and a systematic study of lignin deposition during sugarcane stem development has also been recently performed [19]. Therefore, in this paper, we report a more extensive and detailed structural characterization of the lignins in sugarcane bagasse and straw. For this purpose, we used powerful analytical methodologies, including the thermal degradative method, analytical pyrolysis coupled to gas chromatography and mass spectrometry (Py-GC/MS), spectroscopic methods such as heteronuclear bidimensional solution-state nuclear magnetic resonance (2D-NMR) spectroscopy, and the diagnostic chemical degradative method, derivatization followed by reductive cleavage (DFRC), to delineate the compositional and structural differences between these two lignins. Such data will help to maximize the exploitation of these important agro-industrial wastes as feedstocks for the production of second-generation bioethanol and other biobased products.

2. Materials and methods

2.1. Samples

The samples of sugarcane bagasse and straw were supplied by a mid-sized ethanol mill located in the neighborhood of the São Pedro dos Ferros city, in the same-named County, in Minas Gerais State, Brazil. Sugarcane plants were collected at the approximate age of 6 months from high-performance sugarcane (*Saccharum* spp. hybrids) plantations (UFV/RIDESA RB867515 variety; geographical coordinates are 20° 10′ 0″ South, 42° 31′ 0″ West, altitude of 373 m). This sugarcane cultivar is named following international standard nomenclature, using the alphanumeric designation in which the two first letters indicate the country (RB – Republic of Brazil), the two first numbers (86) indicate the year of hybridization and the last four numbers (7515) indicate the code initially assigned to the clone. The cultivar RB867515 was developed under the scientific cooperation program between UFV (Universidade Federal de Viçosa, Brazil) and RIDESA (Rede Interuniversitária para o Desenvolvimento do Setor Sucroenergético, Brazil), also called UFV/RIDESA [1], and represents 69% of the sugarcane currently planted in Brazil. The sugarcane plants were manually harvested and cleaned in the field where about one-third of their weight was removed in the form of tops, limbs, and foliage; this material is generically called straw throughout this study. The collected straw was immediately transported to the mill in trucks and crushed in a hammer mill in order to homogenize the material well. The remaining two-thirds of the sugarcane plants (stalks), comprised of the sugar itself (one-third = juice = sucrose) and bagasse (one third = crushed stalks) were collected by suitable machines and immediately transported by truck to the ethanol mill. The processing of sugarcane stalks involved two steps. The first was the crushing in a semi-industrial chipper, with the fragments being processed by milling to extract the juice. The resulting residue (bagasse) was used for subsequent characterization studies. Sugarcane bagasse and straw samples were transported to the laboratory where they were air-dried and milled using an IKA knife mill (Janke & Kunkel, Staufen, Germany) and then stored in wide-mouth glass jars until required for analysis.

The contents of acetone-extractives and water-soluble material

Table 1
Abundance (percentage) of the main constituents of the dry weight of sugarcane (*Saccharum spp.*) bagasse and straw.

	Sugarcane bagasse[a]	Sugarcane straw[a]
Water-soluble material	1.3 ± 0.2	2.1 ± 0.2
Acetone extractives	0.9 ± 0.1	1.4 ± 0.1
Klason lignin[b]	17.8 ± 0.6	17.0 ± 0.2
Acid-soluble lignin	2.2 ± 0.2	1.9 ± 0.2
Holocellulose (α-cellulose)[c]	75.8 ± 0.5 (40.1 ± 0.2)	72.9 ± 0.7 (37.9 ± 0.3)
Ash	2.0 ± 0.1	4.7 ± 0.5

[a] Average of three replicates.
[b] Corrected for proteins and ash.
[c] The α-cellulose contents are shown in parentheses.

were measured by extracting ~50 g of sugarcane bagasse or straw with acetone in a Soxhlet for 16 h and then with hot water at 100 °C for 3 h. The lignin content (estimated as Klason lignin) was measured gravimetrically as the insoluble residue from the sulfuric acid hydrolysis of the pre-extracted material according to the TAPPI method T222 om-98 [20]. The Klason lignin content was then corrected for ash, and for protein as determined from the mass fraction of atomic nitrogen obtained by CHN elemental analysis in a LECO CHNS-932 Elemental Analyzer (LECO Corp., St. Joseph, Mich.) and using a 6.25 factor [21]. After filtration of the insoluble lignin, the content of acid-soluble lignin was measured by UV-spectroscopic determination at 205 nm using 11,000 m^2 kg^{-1} as the extinction coefficient, according to Tappi method UM 250 [20]. The content of α-cellulose and hemicelluloses was determined after isolation of the holocellulose from pre-extracted samples by delignification for 4 h using the acid chlorite method [22]. The content of α-cellulose was determined after removing the hemicelluloses by alkaline extraction [22]. Finally, the ash content was estimated as the residue after 6 h of heating at 575 °C under air in a muffle furnace. Three replicates were used for each sample.

2.2. Ball milling and isolation of 'milled-wood' lignins (MWLs)

The MWLs were obtained according to the classical Björkman procedure [23]. Around 40 g of extractive-free material were finely ball-milled in a Retsch PM100 planetary ball mill (Restch, Haan, Germany) at 6.67 Hz (36 h) using an agate jar and 20 spheroid agate balls of 2 cm diameter (this ball-milled material was used directly for whole-cell-wall-NMR to determine compositional and structural features of the entire lignin fraction). The ball-milled material was then extracted with dioxane-water, 96:4 (v/v) (20 cm^3 of solvent/g of milled fiber), and the isolated MWL was subsequently purified as described elsewhere [24]. The final yields ranged from 10 to 15% of the original Klason lignin content.

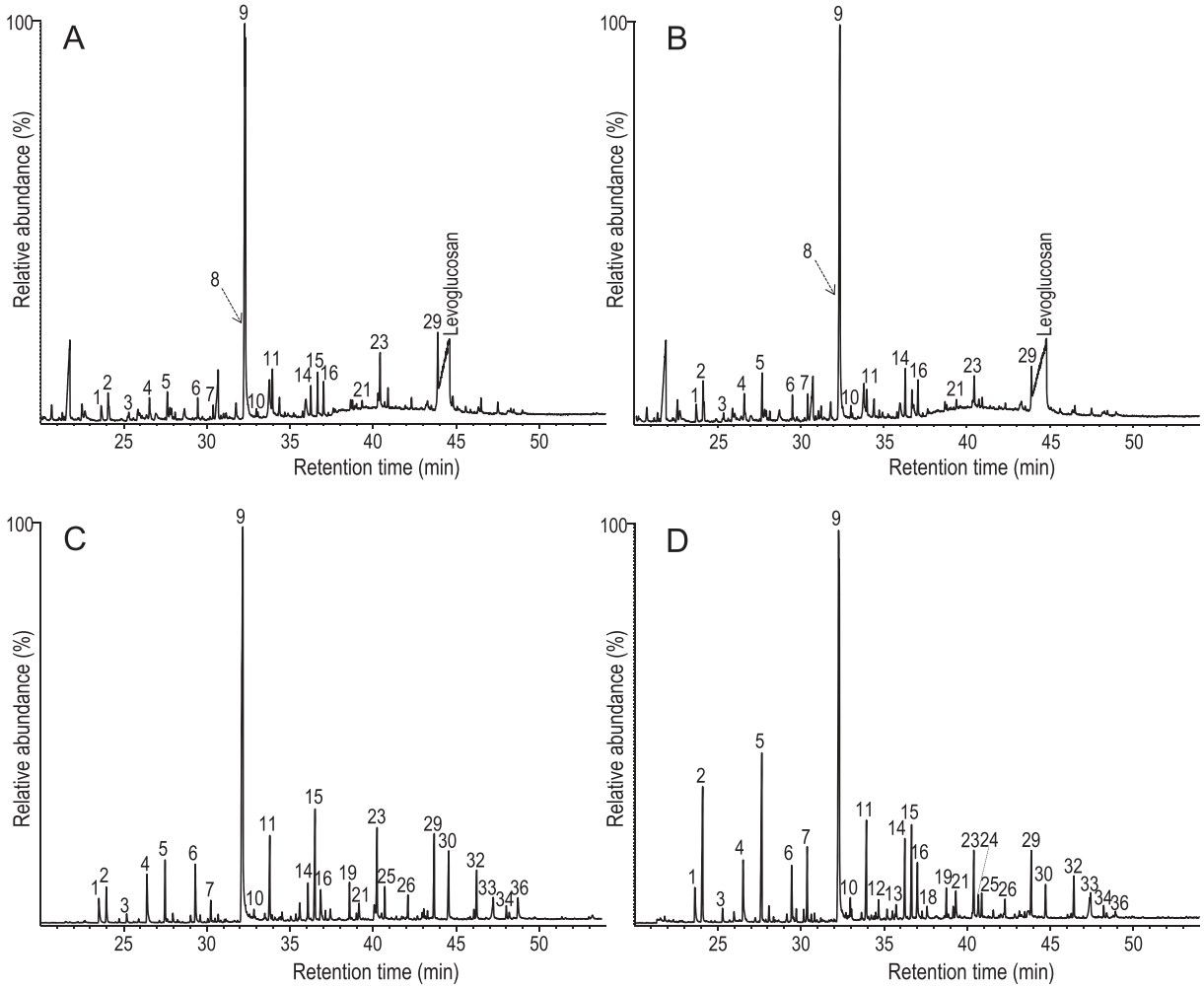

Fig. 1. Py-GC/MS chromatograms of the whole cell-walls of sugarcane (**A**) bagasse and (**B**) straw, and of the MWLs from sugarcane (**C**) bagasse and (**D**) straw. The identities and relative abundances of the released phenolic compounds are listed in Table 2. Levoglucosan arises from carbohydrates.

Table 2
Identities and relative molar abundances of the compounds released after Py-GC/MS of whole cell-walls (CW) of sugarcane (*Saccharum spp.*) bagasse and straw and their isolated MWLs.

	Compounds	Sugarcane bagasse		Sugarcane straw	
		CW	MWL	CW	MWL
1	Phenol	2.4	2.7	3.1	3.0
2	Guaiacol	2.5	2.2	3.9	8.0
3	3-methylphenol	1.0	0.7	1.1	0.8
4	4-methylphenol	2.4	4.2	3.1	4.4
5	4-methylguaiacol	2.3	3.0	4.0	8.9
6	4-ethylphenol	1.4	3.7	2.1	2.9
7	4-ethylguaiacol	0.8	1.0	1.8	2.8
8	4-vinylguaiacol	10.7	3.3	17.0	8.7
9	4-vinylphenol	51.8	41.7	43.8	30.0
10	Eugenol	0.4	0.3	0.8	0.8
11	Syringol	3.0	4.2	2.1	4.3
12	*cis*-isoeugenol	0.3	0.3	0.5	0.7
13	*trans*-4-propenylphenol	0.5	1.0	0.5	0.8
14	*trans*-isoeugenol	1.7	1.5	3.1	3.0
15	4-methylsyringol	2.3	5.1	1.7	3.5
16	Vanillin	2.3	1.9	2.6	2.5
17	Propynylguaiacol	0.2	0.4	0.2	0.3
18	Propynylguaiacol	0.3	0.5	0.3	0.6
19	4-ethylsyringol	0.5	1.2	0.3	0.9
20	Vanillic acid methyl ester	0.0	0.3	0.0	0.4
21	Acetovanillone	0.5	0.9	0.8	1.3
22	4-hydroxybenzaldehyde	0.0	1.3	0.0	0.3
23	4-vinylsyringol	2.9	4.0	1.9	2.5
24	Guaiacylacetone	0.2	0.2	0.5	0.8
25	4-allylsyringol	0.8	1.1	0.6	0.7
26	*cis*-4-propenylsyringol	0.5	0.8	0.3	0.6
27	Propynylsyringol	0.4	0.3	0.4	0.0
28	Propynylsyringol	0.4	0.3	0.2	0.0
29	*trans*-4-propenylsyringol	4.8	3.2	2.0	2.1
30	Syringaldehyde	0.6	3.2	0.0	1.3
31	Syringic acid methyl ester	0.1	0.3	0.1	0.1
32	Acetosyringone	0.6	1.8	0.4	1.4
33	Syringylacetone	0.6	1.2	0.4	0.9
34	Propiosyringone	0.2	0.4	0.1	0.3
35	Syringyl vinyl ketone	0.2	0.3	0.2	0.1
36	*trans*-coniferaldehyde	0.2	1.3	0.3	0.2
37	*trans*-sinapaldehyde	0.3	0.3	0.0	0.0
	S/G ratio[a]	1.3	1.6	0.5	0.5

[a] All G- and S-derived peaks were used for the estimation of the S/G molar ratio, except for 4-vinylguaiacol (peak 8, which also, and predominantly, arises from ferulates), and the analogous 4-vinylsyringol (peak 23).

2.3. Pyrolysis coupled to gas chromatography and mass spectrometry (Py-GC/MS)

Pyrolysis of the whole-cell-walls and of their isolated MWLs (ca. 0.1 mg) was performed at 500 °C in an EGA/PY-3030D micro-furnace pyrolyzer (Frontier Laboratories Ltd., Fukushima, Japan) connected to a GC 7820A (Agilent Technologies, Inc., Santa Clara, CA) and an Agilent 5975 mass-selective detector (EI at 70 eV). The column used was a 60 m × 0.25 mm i.d., 0.25 μm film thickness, DB-1701 (J&W Scientific, Folsom, CA). The oven temperature was programmed from 45 °C (4 min) to 280 °C (10 min) at 4 K min^{-1}. The carrier gas was Helium (2 cm^3 min^{-1}). For the pyrolysis in the presence of tetramethylammonium hydroxide (Py/TMAH), around 0.1 mg of sample was mixed with 0.5 mm^3 of TMAH (25%, w/w, in methanol), the pyrolysis was carried out at 500 °C, and the released products analyzed as described above. Identification of the released compounds was made by comparison of their mass spectra with those of the Wiley and NIST libraries and with those reported in the literature [25] and, when possible, by comparison with the retention times and mass spectra of authentic standards. Molar peak areas were calculated for each lignin degradation product released, the summed areas were normalized, and the data for two replicates were averaged and expressed as percentages.

2.4. Nuclear magnetic resonance (NMR) spectroscopy

2D-NMR spectra (heteronuclear single-quantum coherence, HSQC, and heteronuclear multiple-bond correlation, HMBC) experiments were recorded on an AVANCE III 500 MHz instrument (Bruker, Karlsruhe, Germany) at the NMR facilities of the General Research Services of the University of Seville. For the NMR of the whole-cell-walls of sugarcane bagasse and straw, around 50 mg of finely divided (ball-milled) extractive-free samples were swollen in 0.75 cm^3 DMSO-d_6 according to the method previously described [26,27]. In the case of the isolated MWLs, around 40 mg of underivatized or acetylated sample were dissolved in 0.75 cm^3 of DMSO-d_6 or 0.75 cm^3 of $CDCl_3$, respectively. The central solvent peaks were used as internal references (δ_C/δ_H 39.5/2.49 for DMSO and 70.0/7.26 for $CDCl_3/CHCl_3$). The detailed NMR experimental conditions have been described elsewhere [28]. HSQC cross-signals were assigned by comparison with literature data [24,26–31]. A semi-quantitative analysis of the volume integrals of the HSQC cross-correlation signals was performed as previously described [28].

2.5. Derivatization followed by reductive cleavage (DFRC)

The DFRC degradation was performed according to the method previously developed by Lu and Ralph [32–34], and the detailed explanation of the experimental protocol can be found elsewhere [24,28]. Briefly, around 5 mg of lignin samples were stirred for 2 h at 50 °C with acetyl bromide in acetic acid, 8:92 (v/v) and then treated with powdered Zn (50 mg) for 40 min at room temperature. The lignin degradation products were then acetylated for 1 h in 1.1 cm^3 of dichloromethane containing 0.2 cm^3 of acetic anhydride and 0.2 cm^3 of pyridine. The acetylated lignin degradation products were analyzed by GC/MS using mass spectra and relative retention times to authenticate the DFRC monomers and their *p*-coumarate conjugates as described [32–34]. In order to assess the presence of naturally acetylated lignin units, the DFRC method modified to use propionylating reagents (so-called DFRC′) was used, as previously described [35,36].

The lignin degradation products obtained after DFRC and DFRC′ were analyzed using a GCMS-QP2010plus instrument (Shimadzu Co., Kyoto, Japan) using a capillary column (DB-5MS 30 m × 0.25 mm I.D., 0.25 μm film thickness). The oven was heated from 140 °C (1 min) to 250 °C at 3 K min^{-1}, then ramped at 10 K min^{-1} to 280 °C (1 min) and finally ramped at 20 K min^{-1} to 300 °C, and held for 18 min at the final temperature. The injector was set at 250 °C and the transfer line was kept at 310 °C. The carrier gas was Helium at a rate of 1 cm^3 min^{-1}. Quantitation of the released (acetylated and propionylated) monomers was performed using tetracosane as internal standard and by assuming response factors similar to those of the acetylated monomers reported previously [32]. The molar yields of the released lignin degradation products were determined on the basis of the molecular weights of the respective acetylated or propionylated compounds.

3. Results and discussion

3.1. Composition of the main constituents of sugarcane bagasse and straw

The abundances of the main constituents (water-soluble material, acetone extractives, Klason lignin, acid-soluble lignin, holocellulose, α-cellulose, and ash) of the sugarcane bagasse and straw samples selected for this study are shown in Table 1. The composition is in the range of values previously published for similar samples, except for the much higher content of extractives reported in previous papers [6,37]. However, those papers used 95%

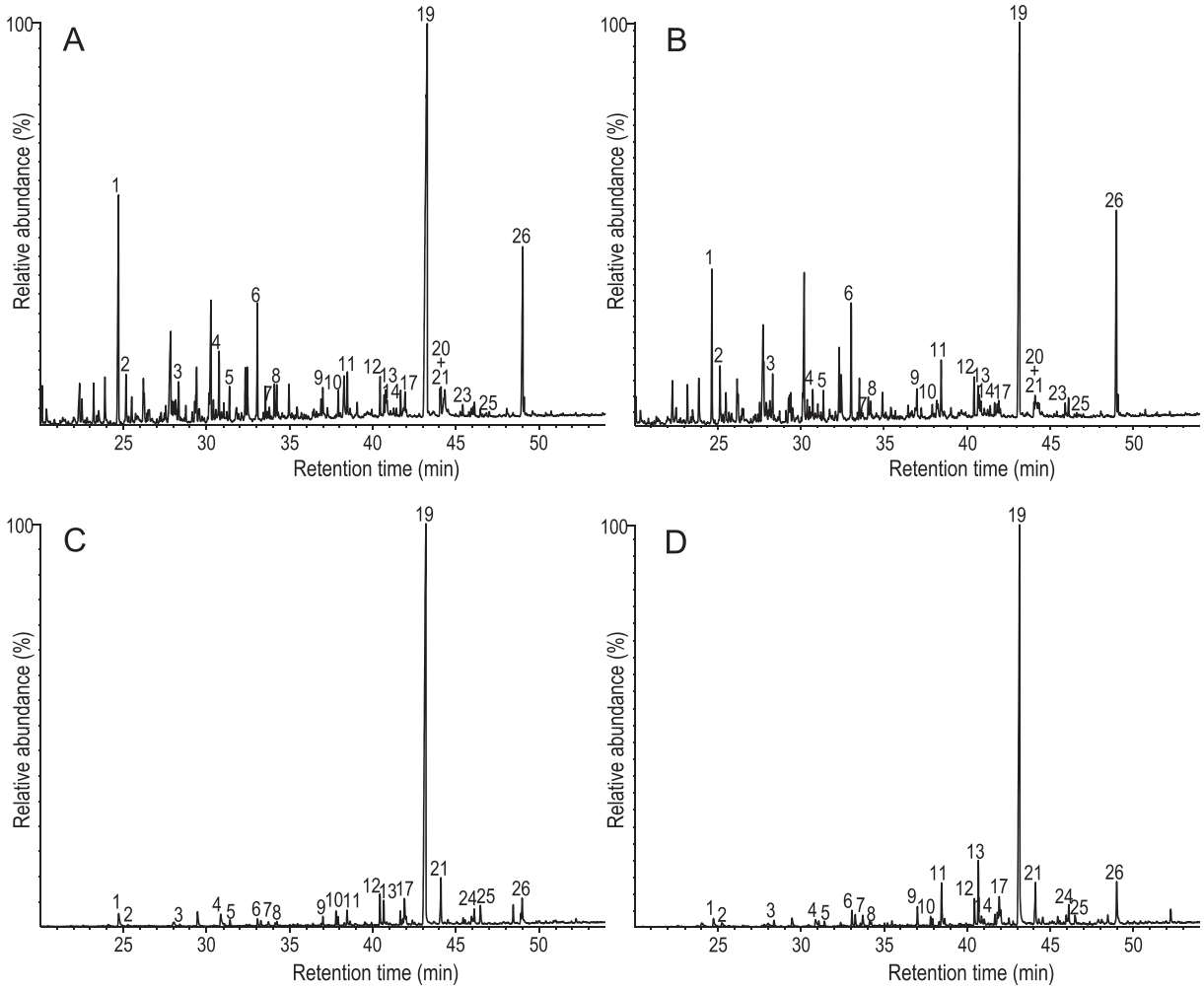

Fig. 2. Py-TMAH-GC/MS chromatograms of the whole cell-walls of sugarcane (**A**) bagasse and (**B**) straw, and of the MWLs from sugarcane (**C**) bagasse and (**D**) straw. The identities and relative abundances of the released compounds are listed in Table 3.

ethanol as solvent, which extracts more polar compounds; in addition, some papers also included the water-soluble material in the total extractives content, thus resulting in higher values. The bagasse and straw samples have a high content of carbohydrates (75.8% and 72.9%) and substantial lignin contents (20% and 18.9%). However, it is worth noting that this composition may vary depending of the cultivar, crop location, year of harvesting, and age of the crop plants, as well as depending of other environmental and cultivation conditions. In this work, the composition of the lignins in both sugarcane residues was analyzed *in situ* by Py-GC/MS and 2D-NMR. To obtain cleaner lignin spectra, MWLs were isolated from the sugarcane residues using a classical lignin isolation protocol [23] and analyzed by Py-GC/MS, 2D-NMR and DFRC.

3.2. Lignin composition of sugarcane bagasse and straw as determined by Py-GC/MS

The whole-cell-walls of sugarcane bagasse and straw and their respective MWLs were first analyzed by Py-GC/MS (Fig. 1). The identities of the released phenolic compounds and their relative molar abundances are listed in Table 2. Pyrolysis released compounds derived from carbohydrates as well as phenolic compounds derived from lignin and from *p*-hydroxycinnamates. Among the phenolics released, the pyrograms showed compounds derived from the H, G and S lignin units such as guaiacol **2**, 4-methylphenol **4**, 4-methylguaiacol **5**, syringol **11**, 4-methylsyringol **15**, 4-vinylsyringol **23** and *trans*-4-propenylsyringol **29**. High amounts of 4-vinylphenol **8** and 4-vinylguaiacol **9** were also released but, as usually occurs in the pyrolysis of grasses, they mostly arise from *p*-coumarates and ferulates after decarboxylation [24,28,38,39]. Pyrolysis of the isolated MWLs released a similar distribution of phenolic compounds except for the much lower relative abundances of 4-vinylguaiacol **8**; this compound is largely derived from ferulates that are attached to polysaccharides and is therefore essentially absent from the MWLs. The most prominent compound released was 4-vinylphenol **9**, derived essentially from *p*-coumarate esters on MWL.

p-Hydroxycinnamates esterify to polysaccharides and/or lignin and are particularly abundant in grasses [15,40–43]. As their efficiently released pyrolysis products can be conflated with those from lignins, care must be exercised when estimating the lignin composition by pyrolysis. *p*-Coumarate- and ferulate-derived 4-vinylphenol and 4-vinylguaiacol were therefore not used for the evaluation of the lignin H:G:S composition. The analysis revealed strong differences in the composition of both lignins, with the lignin of bagasse being S-rich (S/G molar ratio of 1.3–1.6) and the lignin in straw being G-rich (S/G molar ratio of 0.5) (Table 2). This is fairly readily explained by the average maturity of the tissues in each as mature material is always richer in S-units; bagasse is mainly derived from the mature stems, whereas the straw includes the leaves and other immature parts of the plant.

The occurrence of *p*-hydroxycinnamates in sugarcane bagasse

Table 3
Identity and relative molar abundances of the compounds released after Py/TMAH of whole cell-walls of sugarcane (*Saccharum spp.*) bagasse and straw and their isolated MWLs.

Label	Compound	Bagasse CW	Bagasse MWL	Straw CW	Straw MWL
1	4-methoxystyrene	18.0	3.0	12.3	2.5
2	1,2-dimethoxybenzene	2.7	0.4	4.8	1.3
3	3,4-dimethoxytoluene	1.9	0.3	2.9	1.0
4	4-methoxybenzaldehyde	3.8	2.9	2.3	2.0
5	1,2,3-trimethoxybenzene	1.4	0.6	1.7	0.5
6	3,4-dimethoxystyrene	5.6	0.7	7.6	1.9
7	4-methoxybenzoic acid methyl ester	0.3	0.5	0.6	1.7
8	3,4,5-trimethoxytoluene	1.6	0.4	1.3	0.4
9	1-(3,4-dimethoxyphenyl)-1-propene	1.3	0.8	1.8	1.8
10	3,4,5-trimethoxystyrene	1.0	0.7	0.7	0.6
11	3,4-dimethoxybenzaldehyde	2.1	1.7	3.8	5.2
12	*cis*-3-(4-methoxyphenyl)-propenoic acid methyl ester	1.5	2.7	2.1	2.5
13	3,4-dimethoxybenzoic acid methyl ester	0.8	1.9	1.4	5.4
14	3,4-dimethoxyacetophenone	0.6	0.4	0.8	1.0
15	1-(3,4,5-trimethoxyphenyl)-1-propene	0.9	0.9	0.6	0.8
16	*cis*-1-(3,4-dimethoxyphenyl)-2-methoxyethylene	0.1	0.5	0.3	1.1
17	3,4,5-trimethoxybenzaldehyde	1.0	3.0	0.7	2.9
18	*trans*-1-(3,4-dimethoxyphenyl)-2-methoxyethylene	0.2	0.6	0.4	1.2
19	*trans*-3-(4-methoxyphenyl)-propenoic acid methyl ester	43.8	68.7	38.4	54.8
20	3,4,5-trimethoxyacetophenone	0.9	0.6	0.5	1.5
21	3,4,5-trimethoxybenzoic acid methyl ester	0.8	3.1	0.9	2.6
22	3,4,5-trimethoxyphenyl-2-propanone	0.4	0.4	0.2	0.6
23	*cis*-3-(3,4-dimethoxyphenyl)-propenoic acid methyl ester	0.3	0.0	0.7	0.0
24	*cis*-1-(3,4,5-trimethoxyphenyl)-2-methoxyethylene	0.2	1.2	0.1	1.5
25	*trans*-1-(3,4,5-trimethoxyphenyl)-2-methoxyethylene	0.2	1.7	0.1	0.9
26	*trans*-3-(3,4-dimethoxyphenyl)-propenoic acid methyl ester	8.5	2.3	13.0	4.5
p-Coumarate/Ferulate ratio[a]		5.2	31.1	3.0	12.8

[a] Relative molar abundance of *p*-coumarates (peaks 12 and 19) relative to ferulates (peaks 23 and 26).

and straw was confirmed by pyrolysis in the presence of tetramethylammonium hydroxide (TMAH), a reagent that prevents decarboxylation during pyrolysis and liberates diagnostic methyl esters from the esterified components [38,44]. Fig. 2 shows the Py/TMAH chromatograms of the whole cell-walls of bagasse and straw, and of their respective MWLs. The compounds released and their relative molar abundances are listed in Table 3. In general terms, Py/TMAH induces cleavage of alkyl-aryl ether bonds in lignin and releases the methylated derivatives of hydroxybenzaldehydes (**4**, **11**, **17**), hydroxyacetophenones (**14**, **20**) and hydroxybenzoic acids (**7**, **13**, **21**), among others [38,44,45]. As is consistent with the comments above regarding the derivation of 4-vinylphenol and 4-vinylguaiacol from the hydroxycinnamates, Py/TMAH of the whole cell-walls released high amounts (43.8% and 38.4% of the total molar peak areas in bagasse and straw) of the fully methylated derivative of *p*-coumaric acid, the *trans*-3-(4-methoxyphenyl)-propenoic acid methyl ester **19**, as well as significant amounts (8.5% and 13%) of the fully methylated derivative of ferulic acid, the *trans*-3-(3,4-dimethoxyphenyl)-propenoic acid methyl ester **26**. Py/TMAH of the isolated MWLs released higher relative amounts of *p*-coumarate derivatives (68.7% and 54.8% from bagasse and straw), and considerably lower amounts of the ferulate derivatives (2.3% and 4.5%). *p*-Coumarates and ferulates were therefore present in important amounts in the whole cell-walls, with a *p*-coumarate/ferulate molar ratio of 5.2 and 3.0, respectively (Table 3). However, this ratio sharply increases to 31.1 and 12.8 in the MWLs, indicating that in both fractions, ferulates are mostly attached to the carbohydrates in the cell-wall whereas *p*-coumarates are primarily attached to the lignin polymer, as also occurs in other grasses [15]. Previous studies have shown that *p*-coumarates in plants, including grasses, primarily acylate the γ-OH of the lignin side-chain, and predominantly on S-units, whereas ferulates acylate cell-wall polysaccharides and participate in both polysaccharide–polysaccharide and lignin-polysaccharide cross-coupling reactions [15,31,40–43,46].

3.3. Lignin structural units and inter-unit linkages in sugarcane bagasse and straw as elucidated by 2D-NMR

Additional information regarding the structural characteristics of the lignins is available from 2D-NMR analysis of the whole-cell-walls and their isolated MWLs. The HSQC spectra of the whole cell-walls were acquired by swelling finely ball-milled samples in DMSO-d_6 and forming a gel in the NMR tube according to the method previously published [26,27], Figs. 3 and 4. Carbohydrate signals from xylans (X_2, X_3, X_4, X_5), including acetylated xylans (X'_2 and X'_3), were predominant in the aliphatic side-chain region of the whole-cell-wall spectra, partially overlapping with lignin signals. The spectra of the isolated MWLs, however, exhibited predominantly lignin signals that matched those present in the HSQC spectra of their respective whole-cell-walls but that are better resolved. The lignin and carbohydrate cross-signals assigned in the HSQC spectra are listed in Table 4 and the main lignin substructures are drawn in Fig. 5.

In addition to the commonly observed lignin structural units (Fig. 5), the occurrence of intense signals in the range δ_C/δ_H 62.7/3.83–4.30, assigned to the C_γ/H_γ correlations of γ-acylated units (**A′**), revealed that the lignins from sugarcane bagasse and straw are extensively acylated at the γ-position of the lignin side-chain. The extent of lignin acylation was estimated in the HSQC spectra of the isolated MWLs (where the signals from carbohydrates do not interfere) by integration of the C_γ/H_γ signals from the normal (γ-OH) and the γ-acylated lignin units and varied from 42% in the bagasse lignin to 36% in the straw lignin (Table 5), significantly higher than the 10.6% previously reported [18]. The aliphatic side-chain region of the spectra also showed other prominent signals corresponding to the C_α/H_α and C_β/H_β correlations of β–*O*–4′ substructures (**A**, **A′**). Interestingly, the HSQC spectrum of the MWL from the straw showed the presence of a signal at δ_C/δ_H 80.8/4.58 (that was absent in the bagasse) characteristic for the C_β/H_β correlations of γ-acylated β–*O*–4′ substructures **A′** linked to G-

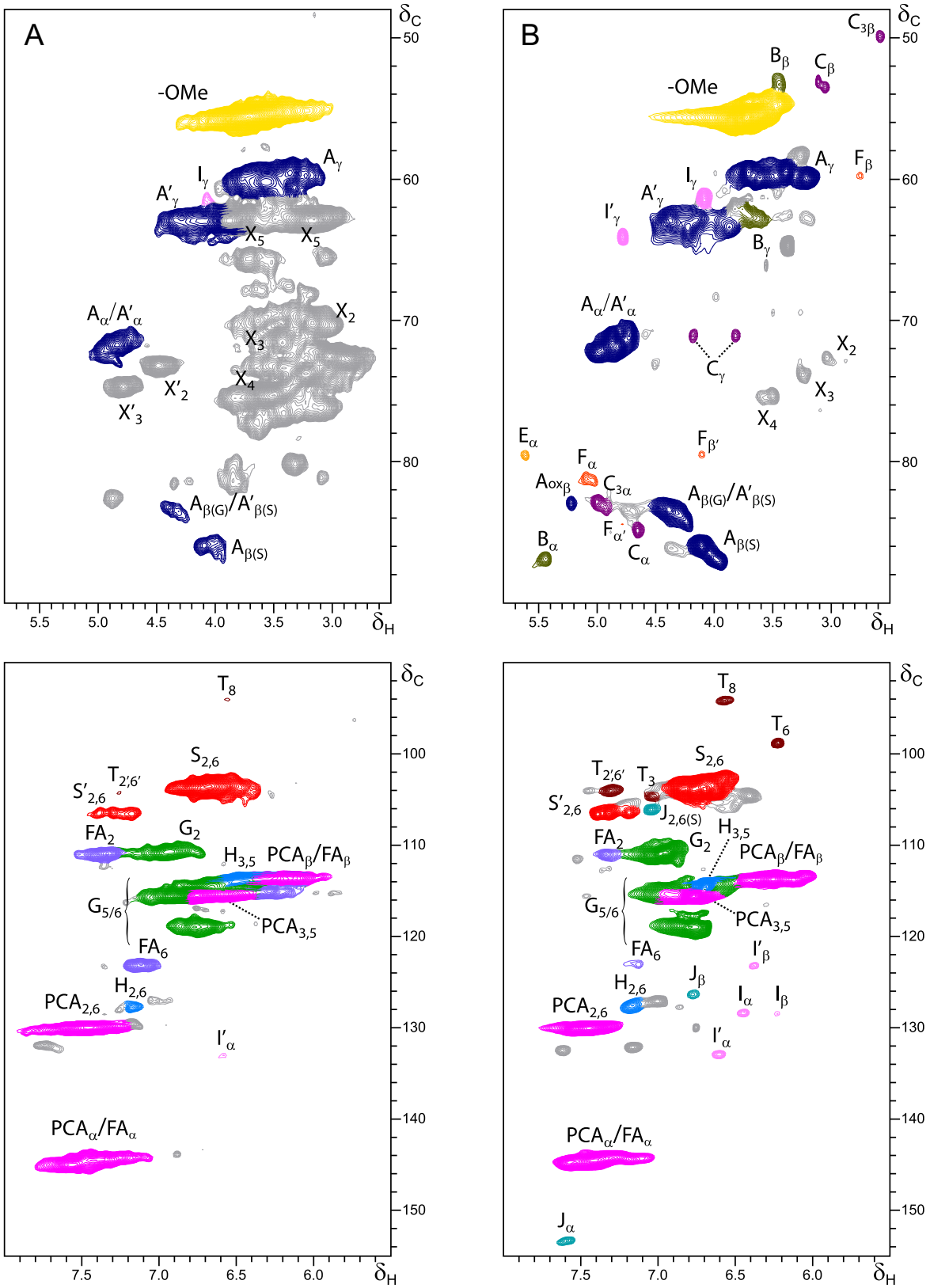

Fig. 3. Side-chain (δ_C/δ_H 48–90/2.5–5.8, top) and aromatic (δ_C/δ_H 90–155/5.5–8.0, bottom) regions from the 2D HSQC NMR spectra of the whole cell-walls from (**A**) sugarcane bagasse and (**B**) its isolated MWL. See Table 4 for signal assignments and Fig. 5 for the main lignin structures identified.

units [24,28], indicating a significant degree of γ-acylation of G-lignin units in the straw lignin.

Signals from other lignin substructures were also observed in the HSQC spectra, being more evident in the isolated MWLs, and included signals for phenylcoumarans **B**, resinols **C**, dibenzodioxocins **D** and spirodienones **F**. Signals for α,β-diaryl ethers **E** could

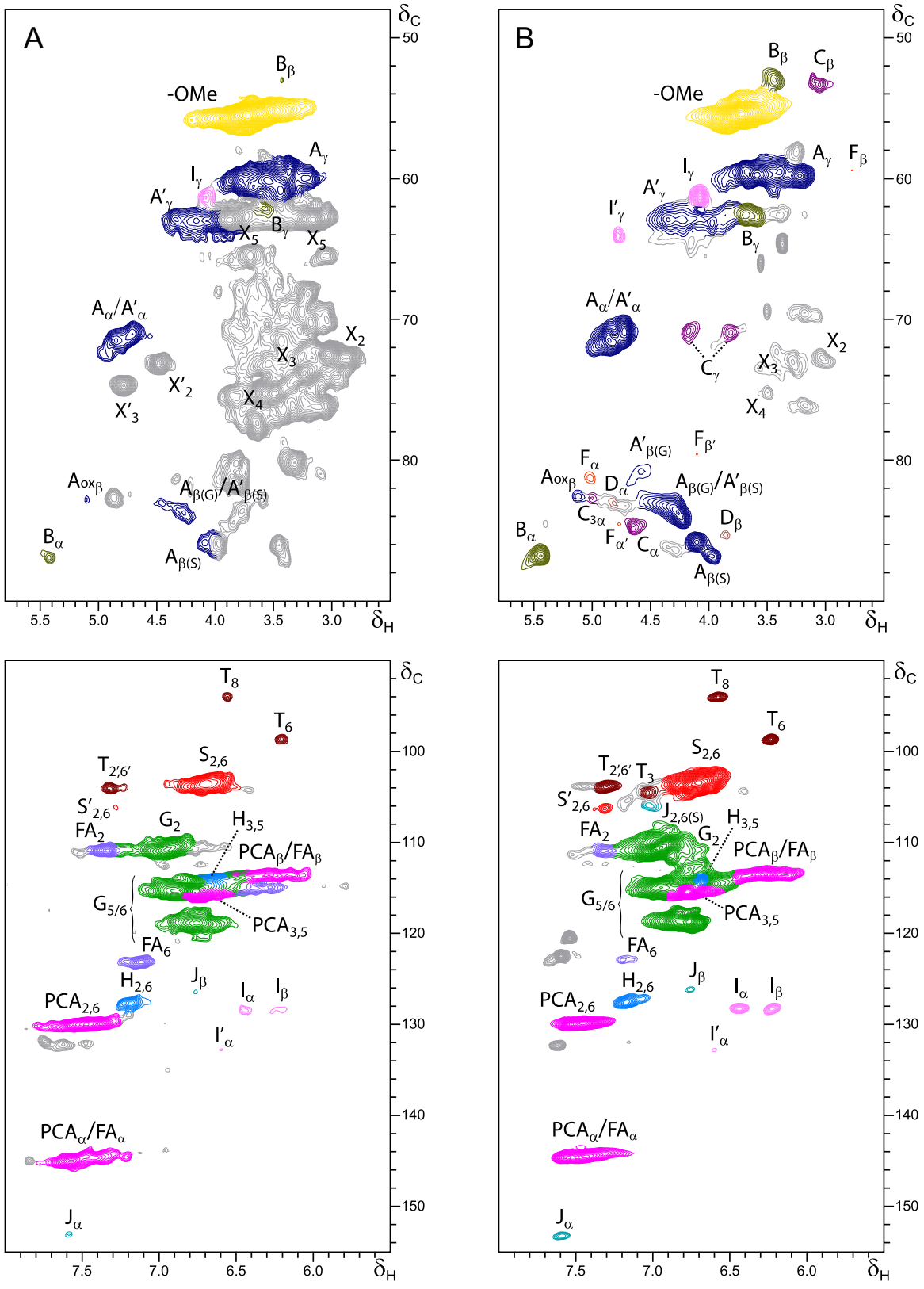

Fig. 4. Side-chain (δ_C/δ_H 48–90/2.50–5.80, top) and aromatic (δ_C/δ_H 90–155/5.50–8.00, bottom) regions from the 2D HSQC NMR spectra of the whole cell-walls from (**A**) sugarcane straw and (**B**) its isolated MWL. See Table 4 for signal assignments and Fig. 5 for the main lignin structures identified.

also be detected in the HSQC of the MWL from bagasse, although with low intensities, as revealed by the C_α/H_α correlation at δ_C/δ_H 79.5/5.50, but were absent in the MWL from straw. In addition, signals for a β–β′ coupled tetrahydrofuran substructure **C$_3$**, arising from β–β′ coupling of two γ-acylated sinapyl alcohols, were observed in the HSQC spectrum of the MWL from bagasse, and in

Table 4
Assignments of $^{1}H/^{13}C$ correlation signals in the 2D HSQC spectra from the whole-cell-walls of sugarcane (*Saccharum spp.*) bagasse and straw and their isolated MWLs in DMSO-d_6.

Label	δ_C/δ_H (ppm)	Assignment
Lignin cross-peak signals		
$C_{3\beta}$	49.8/2.59	C_β/H_β in γ-acylated β–β′ tetrahydrofuran substructures (**C_3**)
B_β	53.6/3.47	C_β/H_β in β–5′ phenylcoumaran substructures (**B**)
C_β	53.6/3.07	C_β/H_β in β–β′ resinol substructures (**C**)
$-OCH_3$	55.6/3.73	C/H in methoxyls
A_γ	59.4/3.40 and 3.72	C_γ/H_γ in normal (γ-hydroxylated) β–*O*–4′ substructures (**A**)
F_β	59.7/2.76	C_β/H_β in spirodienone substructures (**F**)
I_γ	61.3/4.09	C_γ/H_γ in cinnamyl alcohol end-groups (**I**)
B_γ	62.6/3.68	C_γ/H_γ in β–5′ phenylcoumaran substructures (**B**)
A'_γ	62.7/3.83–4.30	C_γ/H_γ in γ-acylated β–*O*–4′ substructures (**A′**)
I'_γ	64.0/4.79	C_γ/H_γ in γ-acylated cinnamyl alcohol end-groups (**I′**)
C_γ	71.0/3.83 and 4.19	C_γ/H_γ in β–β′ resinol substructures (**C**)
A_α/A'_α	71.8/4.87	C_α/H_α in β–*O*–4′ substructures (**A, A′**)
$F_{\beta'}$	79.5/4.11	$C_{\beta'}/H_{\beta'}$ in spirodienone substructures (**F**)
E_α	79.5/5.50	C_α/H_α in α,β-diaryl ether substructures (**E**)
$A'_{\beta(G)}$	80.8/4.58	C_β/H_β in γ-acylated β–*O*–4′ substructures linked to a G unit (**A′**)
F_α	81.2/5.10	C_α/H_α in spirodienone substructures (**F**)
$C_{3\alpha}$	82.8/5.00	C_α/H_α in γ-acylated β–β′ tetrahydrofuran structures (**C_3**)
$A_{ox\beta}$	82.8/5.23	C_β/H_β in α-oxidized β–*O*–4′ substructures (**A_{ox}**)
$A'_{\beta(S)}$	83.0/4.33	C_β/H_β in γ-acylated β–*O*–4′ substructures linked to an S unit (**A′**)
D_α	83.4/4.82	C_α/H_α in 5-5′ dibenzodioxocin substructures (**D**)
$A_{\beta(G)}$	83.6/4.29	C_β/H_β in β–*O*–4′ substructures linked to a G unit (**A**)
C_α	84.8/4.67	C_α/H_α in β–β′ resinol substructures (**C**)
$F_{\alpha'}$	84.9/4.88	$C_{\alpha'}/H_{\alpha'}$ in spirodienone substructures (**F**)
D_β	85.4/3.86	C_β/H_β in 5-5′ dibenzodioxocin substructures (**D**)
$A_{\beta(S)}$	85.9/4.12	C_β/H_β in β–*O*–4′ substructures linked to a S unit (**A**)
B_α	86.9/5.47	C_α/H_α in phenylcoumaran substructures (**B**)
T_8	94.0/6.56	C_8/H_8 in tricin units (**T**)
T_6	98.7/6.22	C_6/H_6 in tricin units (**T**)
$S_{2,6}$	103.8/6.69	C_2/H_2 and C_6/H_6 in etherified syringyl units (**S**)
$T_{2',6'}$	103.9/7.30	$C_{2'}/H_{2'}$ and $C_{6'}/H_{6'}$ in tricin units (**T**)
T_3	104.5/7.03	C_3/H_3 in tricin units (**T**)
$S'_{2,6}$	106.1/7.32 and 106.4/7.19	C_2/H_2 and C_6/H_6 in α-oxidized syringyl units (**S′**)
$J_{2,6(S)}$	106.8/7.06	C_2/H_2 and C_6/H_6 in cinnamaldehyde end-groups in S units (**J**)
G_2	110.9/7.00	C_2/H_2 in guaiacyl units (**G**)
FA_2	111.0/7.32	C_2/H_2 in ferulic acid units (**FA**)
PCA_β and FA_β	113.5/6.27	C_β/H_β in *p*-coumarate (**PCA**) and ferulate (**FA**)
$H_{3,5}$	114.5/6.62	C_3/H_3 and C_5/H_5 in *p*-hydroxyphenyl units (**H**)
G_5/G_6	114.9/6.72 and 6.94 118.7/6.77	C_5/H_5 and C_6/H_6 in guaiacyl units (**G**)
$PCA_{3,5}$	115.5/6.77	C_3/H_3 and C_5/H_5 in *p*-coumarate (**PCA**)
I'_β	123.2/6.38	C_β/H_β in γ-acylated cinnamyl alcohol end-groups (**I′**)
FA_6	123.3/7.10	C_6/H_6 in ferulate (**FA**)
J_β	126.3/6.76	C_β/H_β in cinnamaldehyde end-groups (**J**)
$H_{2,6}$	128.0/7.23	C_2/H_2 and C_6/H_6 in *p*-hydroxyphenyl units (**H**)
I_β	128.4/6.23	C_β/H_β in cinnamyl alcohol end-groups (**I**)
I_α	128.4/6.44	C_α/H_α in cinnamyl alcohol end-groups (**I**)
$PCA_{2,6}$	130.0/7.46	C_2/H_2 and C_6/H_6 in *p*-coumarate (**PCA**)
I'_α	132.9/6.60	C_α/H_α in γ-acylated cinnamyl alcohol end-groups (**I′**)
PCA_α and FA_α	144.4/7.41	C_α/H_α in *p*-coumarate (**PCA**) and ferulate (**FA**)
J_α	153.4/7.61	C_α/H_α in cinnamaldehyde end-groups (**J**)
Polysaccharide cross-peak signals		
X_5	63.2/3.26 and 3.95	C_5/H_5 in β-D-xylopyranoside
X_2	72.9/3.14	C_2/H_2 in β-D-xylopyranoside
X'_2	73.5/4.61	C_2/H_2 in 2-*O*-acetyl-β-D-xylopyranoside
X_3	74.1/3.32	C_3/H_3 in β-D-xylopyranoside
X'_3	74.9/4.91	C_3/H_3 in 3-*O*-acetyl-β-D-xylopyranoside
X_4	75.6/3.63	C_4/H_4 in β-D-xylopyranoside

lower intensities from straw, with their characteristic C_α/H_α and C_β/H_β correlations being at δ_C/δ_H 82.8/5.00 and 49.8/2.59. This tetrahydrofuran structure has also been observed in the lignins from other plants, including other grasses such as elephant grass and corn [24,47]. Other signals in this region of the spectra corresponded to the C_γ/H_γ correlations of cinnamyl alcohol end-groups **I** and γ-acylated cinnamyl alcohol end-groups **I′**, as well as to the C_β/H_β correlations of α-keto- β–*O*–4′ alkyl-aryl ethers (**A_{ox}**).

In the aromatic/unsaturated region of the HSQC spectra are the main correlation signals corresponding to the aromatic rings of the different lignin units (**H**, **G**, **S**), including Cα-oxidized S-lignin units **S′**, as well as to the aromatic rings and the unsaturated side-chains of the *p*-hydroxycinnamates (**PCA**, **FA**). The signals for H-lignin units were only observed in low intensities, confirming that the high amounts of 'H-units' released upon Py-GC/MS were mostly due to *p*-coumarates. In addition, in this region of the HSQC spectra appeared the two distinctive signals at δ_C/δ_H 94.0/6.56 and 98.7/6.22 corresponding to the C_8/H_8 and C_6/H_6 correlations of tricin **T** [28]. Tricin is a flavone that is now widely found, and is apparently incorporated, into the lignin structure in grasses [28,39,48–50] and that also occurs in the lignin of other monocotyledons, such as coconut coir [51]. The HSQC spectra also show the C_3/H_3 correlation of tricin at δ_C/δ_H 104.5/7.03 as well as the correlations for $C_{2'}/H_{2'}$ and $C_{6'}/H_{6'}$ at δ_C/δ_H 103.9/7.30. Other signals in aromatic/

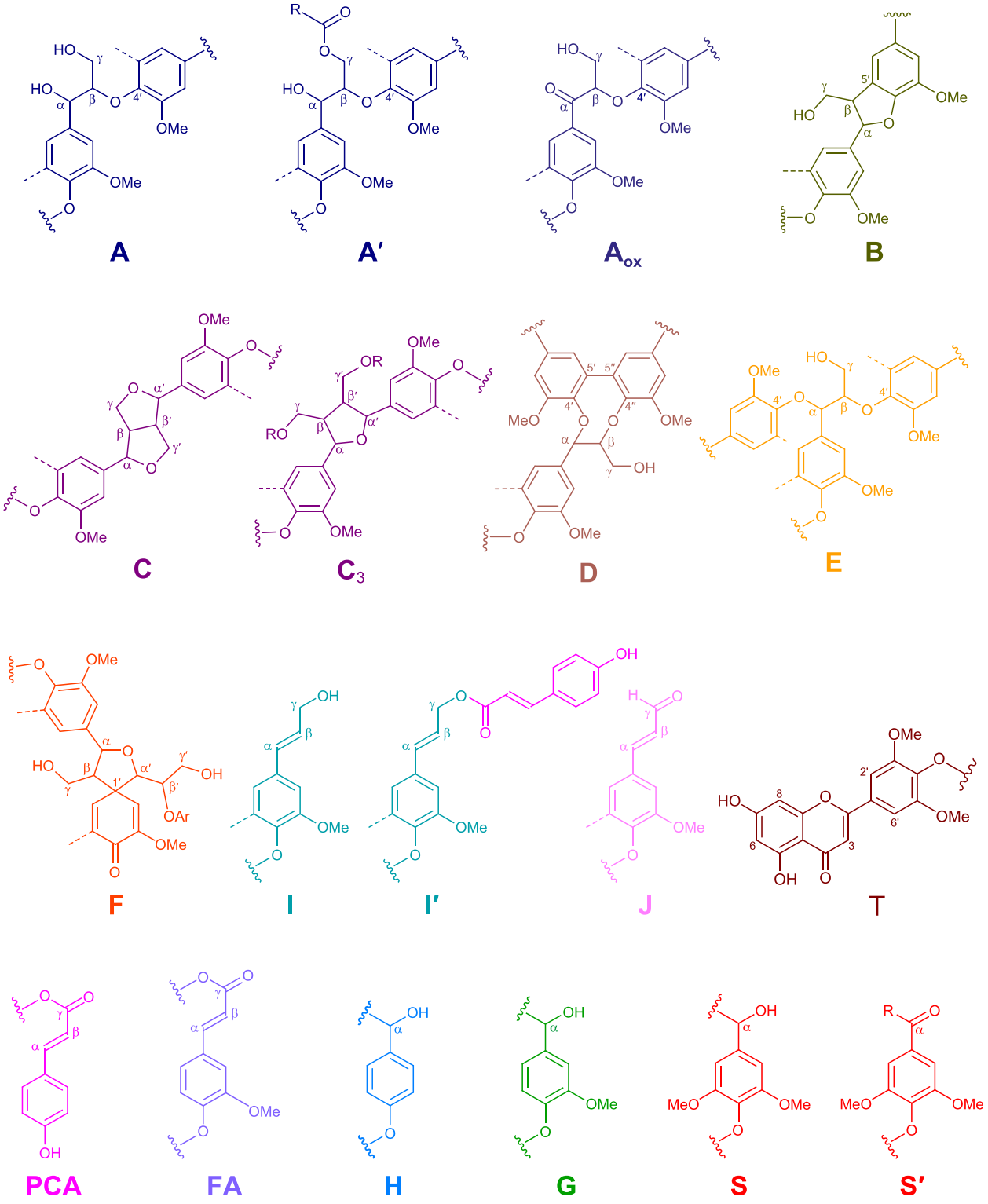

Fig. 5. Main structures present in the lignins of sugarcane bagasse and straw as identified in the NMR spectra of Figs. 3 and 4. **A**: β–*O*–4′-structures; **A′**: β-*O*-4′-structures with acylated (by acetate or *p*-coumarate) γ-OH; **A_{ox}**: C_α-oxidized β–*O*–4′ structures; **B**: phenylcoumaran structures formed by β–5′-coupling; **C**: resinol structures formed by β–β′-coupling; **C_3**: tetrahydrofuran structures formed by β–β′-coupling of monolignols acylated at the γ-OH; **D**: dibenzodioxocin structures formed by 5–5′- followed by 4–O–β-coupling; **E**: α,β-diaryl ether structures; **F**: spirodienone structures formed by β–1′-coupling; **I**: *p*-hydroxycinnamyl alcohol end-groups; **I′**: *p*-hydroxycinnamyl alcohol end-groups acylated at the γ-OH; **J**: cinnamaldehyde end-groups; **T**: tricin end-groups; **PCA**: *p*-coumarate moieties; **FA**: ferulate moieties (esterified with hemicelluloses); **H**: *p*-hydroxyphenyl units; **G**: guaiacyl units; **S**: syringyl units; **S′**: oxidized syringyl units bearing a carbonyl group at Cα. The structures are colored to match the assigned contours in the NMR spectra in Figs. 3 and 4.

unsaturated region of the HSQC spectra are from cinnamyl alcohol end-groups **I** and cinnamaldehyde end-groups **J**. In addition, a signal for the $C_{2,6}/H_{2,6}$ correlation of sinapaldehyde end-groups **J_S**, was observed at δ_C/δ_H 106.8/7.06; however, no aromatic signals for coniferaldehyde end-groups were detected in the spectra. Signals for γ-acylated cinnamyl alcohol end-groups **I′** were also detected

Table 5
Structural characteristics (lignin inter-unit linkage types, end-groups, γ-acylation, aromatic units, and S/G Ratio, cinnamate content and *p*-coumarate/ferulate ratio, and tricin content) from integration of $^{1}H/^{13}C$ correlation signals in the HSQC spectra from the whole cell-walls of sugarcane (*Saccharum spp.*) bagasse and straw and their isolated MWLs.

	Sugarcane bagasse CW	Sugarcane bagasse MWL	Sugarcane straw CW	Sugarcane straw MWL
Lignin inter-unit linkages (%)				
β–*O*–4′ Aryl ethers (**A**/**A**′)	–	80	–	75
α-Oxidized β–*O*–4′ aryl ethers ($\mathbf{A_{ox}}$)	–	3	–	0
Phenylcoumarans (**B**)	–	6	–	15
Resinols (**C**)	–	2	–	3
Tetrahydrofurans ($\mathbf{C_3}$)	–	4	–	1
Dibenzodioxocins (**D**)	–	0	–	3
α,β-diaryl ethers (**E**)	–	2	–	0
Spirodienones (**F**)	–	3	–	3
Lignin end-groups[a]				
Cinnamyl alcohol end-groups (**I**)	–	3	–	7
γ-Acylated cinnamyl alcohol end-groups (**I**′)	–	2	–	3
Cinnamaldehyde end-groups (**J**)	–	4	–	2
Lignin side-chain γ-acylation (%)	–	42	–	36
Lignin aromatic units[b]				
H (%)	3	2	5	4
G (%)	37	38	66	68
S (%)	60	60	29	28
S/G ratio	1.6	1.6	0.4	0.4
p-Hydroxycinnamates[c]				
p-Coumarate (%)	68	48	35	21
Ferulate (%)	26	4	18	5
p-Coumarate/Ferulate ratio	2.6	12.0	1.9	4.2
Tricin[c]	2	2	4	4

[a] Expressed as a fraction of the total lignin inter-unit linkage types **A**–**F.**
[b] Molar percentages (H + G + S = 100).
[c] *p*-Coumarate, ferulate and tricin molar contents (integrals) as percentages of lignin content (H + G + S).

in this region of the spectra, with the characteristic C_α/H_α and C_β/H_β correlations observed at δ_C/δ_H 132.9/6.60 and 123.2/6.38. These signals were particularly evident in the HSQC spectrum of the MWL from bagasse, and derive from its higher extent of γ-acylation, but were present in lower amounts in the HSQC of the MWL from straw, with a lower degree of γ-acylation.

Some authors [18] have also reported the occurrence of *p*-hydroxybenzoates in the lignin from sugarcane bagasse based on the presence of a signal in the HSQC spectra at δ_C/δ_H 132.4/7.63, which is also observed in the HSQC of our samples. However, a close comparison with the HSQC spectra of other lignins from our own collection with proven occurrence of *p*-hydroxybenzoates indicates that this assignment was not correct as the $C_{2,6}/H_{2,6}$ correlation signal for *p*-hydroxybenzoates that should appear around δ_C/δ_H 131.2/7.68 [51] does not match with that signal. The absence of other known correlations in the HMBC spectra also discards this signal as belonging to *p*-hydroxybenzoates. *p*-Hydroxybenzoates have been widely found acylating the γ-OH of the lignin in palms and *Populus* species (willow, aspen, poplar) [47,51–56] but have never been found in grasses, and therefore, in addition to our not observing methylated *p*-hydroxybenzoate in the Py/TMAH analysis, we can dismiss the occurrence of *p*-hydroxybenzoates in the lignins from sugarcane.

The structural characteristics of the lignins from sugarcane bagasse and straw, such as the relative abundances of the different interunit linkages and cinnamyl end-groups, the percentage of γ-acylation, the molar abundances of the lignin units (H, G, and S), *p*-coumarates, ferulates, and tricin, estimated from volume integration of the signals in the HSQC spectra, are indicated in Table 5. The data confirmed the completely different composition of the two lignins noted above from the Py-GC/MS data. The H:G:S molar composition of the lignin from bagasse (2:38:60) was quite different to that from the straw (4:68:28). The S/G molar ratios obtained by 2D-NMR closely matched those determined by Py-GC/MS, indicating a predominance of S units in the lignin from sugarcane bagasse (S/G molar ratio of 1.6) and a predominance of G units in the lignin from sugarcane straw (S/G molar ratio of 0.4). This data also confirms that the content of H-units in the lignins from both sugarcane residues is quite low (<5%, Table 5), and that the high abundance of *p*-hydroxyphenyl compounds observed upon Py-GC/MS was due to pyrolytic decarboxylation of *p*-coumarates. 2D-NMR data indicated that *p*-coumarates are present in high abundance in the whole-cell-walls, as well as in their isolated MWLs, whereas ferulates are present in much lower abundance in the isolated MWLs than in the respective whole-cell-walls, as already observed by Py-GC/MS and Py/TMAH. This is because, as already indicated above, ferulates are primarily attached to the polysaccharides whereas *p*-coumarates are predominantly attached to the lignin. This information, together with the high extent of acylation of the γ-OH of the lignin side-chain observed in these lignins (42% and 36% of lignin acylation in bagasse and straw), seems to indicate that *p*-coumarates are the groups acylating the γ-OH of the lignin side-chain, as has been observed in the lignins of other plants [15,24,28,31,34,40,43,46]. The flavone tricin was also present in both lignins, being more abundant in the straw. Tricin has been suggested to act as a lignin monomer in grasses and its incorporation into the lignin polymer through 4–*O*–β coupling reactions has been indicated [28], and such coupling has been validated in biomimetic coupling reactions [50]. Tricin cannot couple with another tricin molecule, so it can only undergo cross-coupling reactions with monolignols and therefore must be present at the start of a lignin chain; tricin therefore seems to act as a nucleation or initiation site for lignification [28,50].

The differences in composition between the lignins from sugarcane bagasse and straw are also reflected in the differences in the relative abundances of the various interunit linkages between them. Thus, the bagasse lignin is mostly made up of β–*O*–4′ alkyl-aryl ether linkages (accounting for 83% of all the interunit linkage types measured), followed by minor amounts of β–5′ phenylcoumarans (6%) and other condensed units. The straw lignin, on the other hand, has lower levels of β–*O*–4′ alkyl-aryl ether linkages (75% of all the interunit linkages) and has higher amounts of β–5′

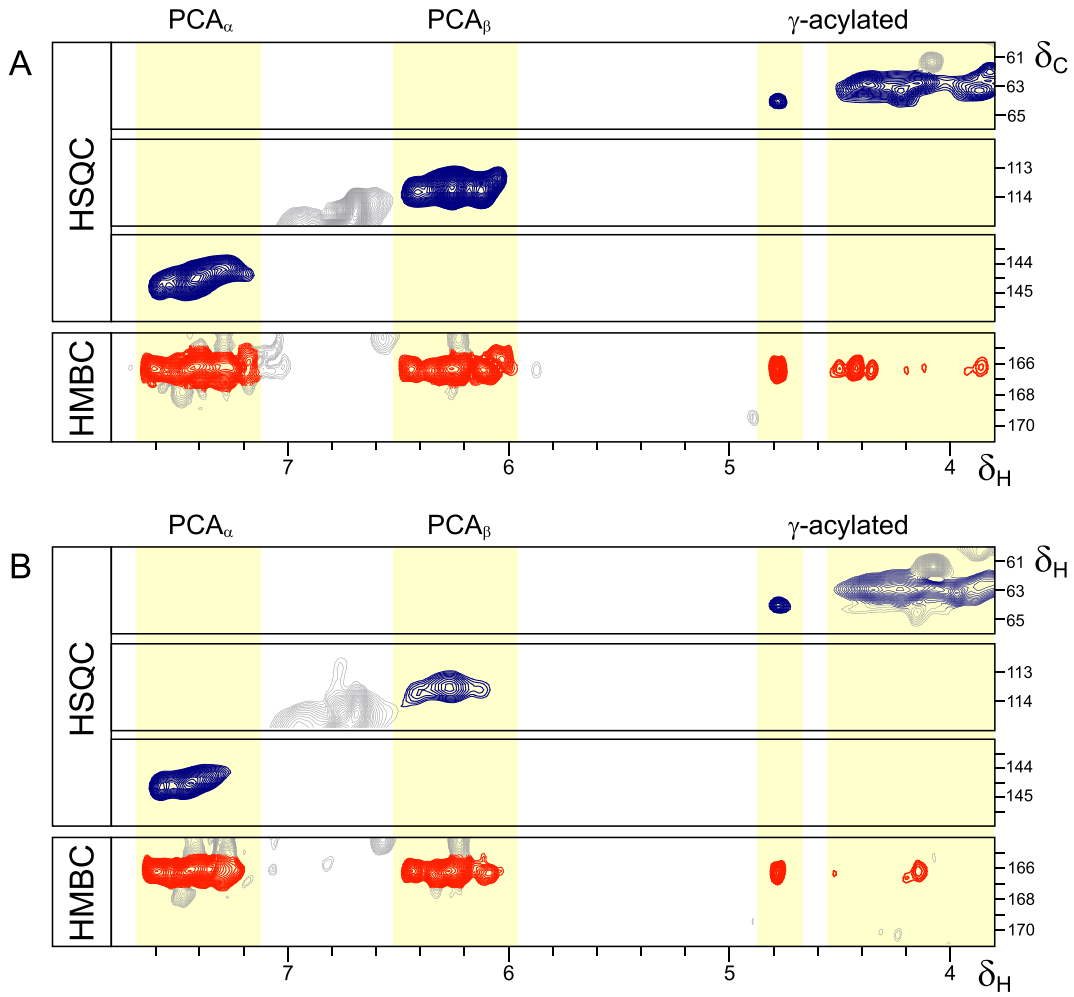

Fig. 6. Sections of the HMBC spectra (δ_C/δ_H 164–171/3.8–7.8) of the MWLs isolated from (**A**) sugarcane bagasse and (**B**) straw showing the main correlations for the carbonyl carbons of *p*-coumarates (PCA) acylating the γ-OH of the lignin side-chains. Appropriate sections of the HSQC spectra showing the C_γ/H_γ correlations of the acylated lignin (δ_C 60–66) and the C_α/H_α and C_β/H_β correlations of *p*-coumarates (δ_C 112–115 and 142–147, respectively), are also depicted. Note the absence of signals for the carbonyl carbons from acetates acylating the γ-position of the lignin side-chains (at δ_C 169.8).

phenylcoumarans (15%) and dibenzodioxocins (3%), as is consistent with a lignin enriched in G-units. Minor amounts of α,β-diaryl ethers (2%) were also found in the bagasse lignin, but were absent from the straw. Other condensed substructures, such as β–β′ resinols and β–1′ spirodienones, are present in minor amounts in both lignins. The unusually low proportions of β–β′ resinol substructures observed in these lignins, accounting for only 2% of all interunit linkages in the bagasse lignin and 3% in the straw lignin, seem to be related to the high extent of acylation of the γ-OH in these lignins, as also noted in other highly acylated lignins [24,31]. This is because the formation of normal β–β′ resinol structures requires a free γ-OH in order to rearomatize the intermediate quinone methide (following the radical dehydrodimerization step). If the γ-OH of a monolignol is acylated, normal resinol structures cannot be formed, and instead, unconventional β–β′ tetrahydrofuran structures are formed from β–β′ homocoupling of two γ-acylated monolignols or from β–β′ cross-coupling of a normal (γ-OH) monolignol with a γ-acylated monolignol [47,55–57]. Interestingly, significant amounts of a β–β′ tetrahydrofuran structure (**C$_3$**) formed by β–β′ homocoupling of two γ-acylated monolignols were found in these lignins, being particularly abundant in the lignin from sugarcane bagasse (4% of all interunit linkages), as is consistent with its higher level of γ-acylation (42% of all side-chains).

3.4. Details of lignin acylation by p-coumarate (and more minor levels of acetate) from 2D-NMR and DFRC

p-Coumarates are widely present in grasses, and in other plants, acylating the γ-OH of the lignin side-chain [15,24,28,31,34,40,43,46]. In order to demonstrate that the *p*-coumarates present in the lignins from sugarcane bagasse and straw are of the same type, we performed 2D-NMR HMBC experiments that correlate protons with carbons separated by 2- or 3-bonds. Fig. 6 shows the MWL HMBC sections for the carbonyl carbon correlations. Strong signals are observed for the *p*-coumarate ester carbonyl correlations at δ_C 166.0 with their α- and β-protons at δ_H 7.41 and 6.27, and with protons in the range δ_H 4.0–4.8 ppm in both HMBC spectra confirming that *p*-coumarate groups acylate the γ-OH of the lignin side-chains, as usually occurs in grasses. The HMBC spectra, however, did not show similar correlations for acetate groups (at δ_C 169.8), despite previous findings that lignin γ-acetates are widely found, including in grasses [24,28,31,35,36,58]. Apparently, the extent of γ-acetylation, if any, is below the detection limit of the HMBC experiment here.

Additional information regarding the nature of the acylation of the γ-OH was obtained from DFRC, a degradation method that cleaves (α- and) β-ether bonds but leaves γ-esters intact [32–34].

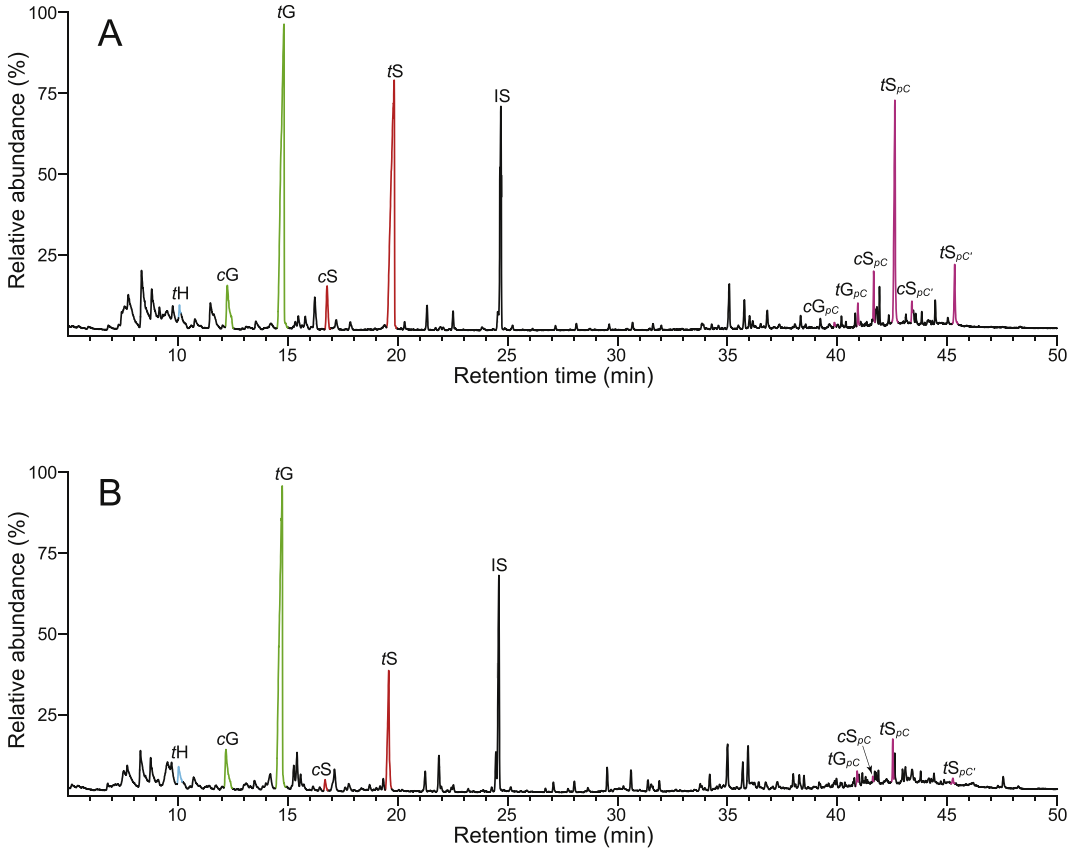

Fig. 7. Chromatograms of the DFRC degradation products from the MWLs isolated from (**A**) sugarcane bagasse and (**B**) straw showing the presence of sinapyl (and minor coniferyl) units acylated by *p*-coumarate moieties. *t*H, *c*G, *t*G, *c*S and *t*S are the normal *cis*- and *trans*-*p*-hydroxyphenyl (H), coniferyl (G) and sinapyl (S) alcohol monomers (as their acetate derivatives). cG_{pC}, tG_{pC}, cS_{pC} and tS_{pC} are the *cis*- and *trans*-coniferyl and sinapyl dihydro-*p*-coumarates (as their acetate derivatives). $cS_{pC'}$ and $tS_{pC'}$ are the *cis*- and *trans*-sinapyl *p*-coumarates (as their acetate derivatives). IS: internal standard (*n*-tetracosane).

Table 6
Abundance (μmol/g of lignin) of the monomers obtained from DFRC degradation of the MWLs from sugarcane (*Saccharum spp.*) bagasse and straw, and relative percentages of the different acylated (acetylated and *p*-coumaroylated) lignin monomers.

	H	G	G_{ac}	G_{pC}	S	S_{ac}	S_{pC}[a]	$\%G_{ac}$[b]	$\%G_{pC}$[c]	$\%S_{ac}$[d]	$\%S_{pC}$[e]
MWL Bagasse	2	128	5	2	98	1	30	3.7	1.5	0.8	23.3
MWL Straw	4	112	4	1	24	0.5	3	3.4	0.8	1.8	10.9

[a] Includes the sum of sinapyl *p*-coumarates (S_{pC}) and sinapyl dihydro-*p*-coumarates ($S_{pC'}$).
[b] $\%G_{ac}$ is the percentage of acetylated G units (G_{ac}) with respect to the total G units (G, G_{ac}, G_{pC}).
[c] $\%G_{pC}$ is the percentage of *p*-coumaroylated G units (G_{pc}) with respect to the total G units (G, G_{ac}, G_{pC}).
[d] $\%S_{ac}$ is the percentage of acetylated S units (S_{ac}) with respect to the total S units (S, S_{ac}, S_{pC}).
[e] $\%S_{pC}$ is the percentage of total *p*-coumaroylated S units (including sinapyl *p*-coumarates, S_{pC}, and sinapyl dihydro-*p*-coumarates, $S_{pC'}$), with respect to the total S units (S, S_{ac}, S_{pC}).

Fig. 7 shows the chromatograms of the DFRC degradation products obtained from the MWLs from sugarcane bagasse and straw. The DFRC of the isolated MWLs produced the *cis*- and *trans*-isomers of the acetylated *p*-hydroxyphenyl (*t*H), guaiacyl (*c*G and *t*G), and syringyl (*c*S and *t*S) lignin monomers arising from normal, non-γ-*p*-coumaroylated β-ether lignin units. In addition, the chromatograms revealed the presence of important peaks corresponding to the *cis*- and *trans*-isomers of S-lignin units acylated with *p*-coumarates. Both saturated (cS_{pC} and tS_{pC}) and unsaturated ($cS_{pC'}$ and $tS_{pC'}$) DFRC-derived products were particularly abundant in the MWL from sugarcane bagasse, together with minor amounts of the guaiacyl analogs (cG_{pC} and tG_{pC}). The release of these compounds confirmed that *p*-coumarate groups are acylating the γ-OH of these lignins, and predominantly on S units, as usually occurs in grasses [15,24,28,31,34,40,43,46]. Because the original DFRC degradation method masked the presence of natural acetates, a modification in which acetylating reagents are substituted for their propionylating counterparts (DFRC′) is used to reveal native lignin acetylation [35,36]. By this method it was possible to detect the presence of minor amounts of γ-acetylated G- and S-lignin units in the MWL isolated from both sugarcane bagasse and straw, demonstrating that native acetylation of the γ-OH also occurred in these lignins, although to a low extent.

Table 6 presents the results from the DFRC and DFRC′ degradations of the MWLs isolated from sugarcane bagasse and straw, including the molar yields of the released monomers (H, G, G_{ac}, G_{pC}, S, S_{ac}, S_{pC}), as well as the percentages of naturally acetylated guaiacyl ($\%G_{ac}$) and syringyl ($\%S_{ac}$) and *p*-coumaroylated guaiacyl ($\%G_{pc}$) and syringyl ($\%S_{pc}$) lignin units (the values for S_{pC} include the sum of both the saturated and the unsaturated *p*-coumarate analogs). The analyses confirm the high level of γ-acylation in the lignin of sugarcane bagasse, that are mostly due to *p*-coumarates that are predominantly attached to S-units (23.3% of the S-units and only 1.5% of G-units are *p*-coumaroylated). Lower amounts of γ-*p*-coumaroylated guaiacyl (0.8%) and syringyl (10.9%) conjugates were released in the DFRC from the MWL from sugarcane straw, despite the substantial amounts of *p*-coumarates present in this lignin (21% with respect to the total lignin aromatic units, as estimated by 2D-NMR, Table 5) and the fact that they are acylating the

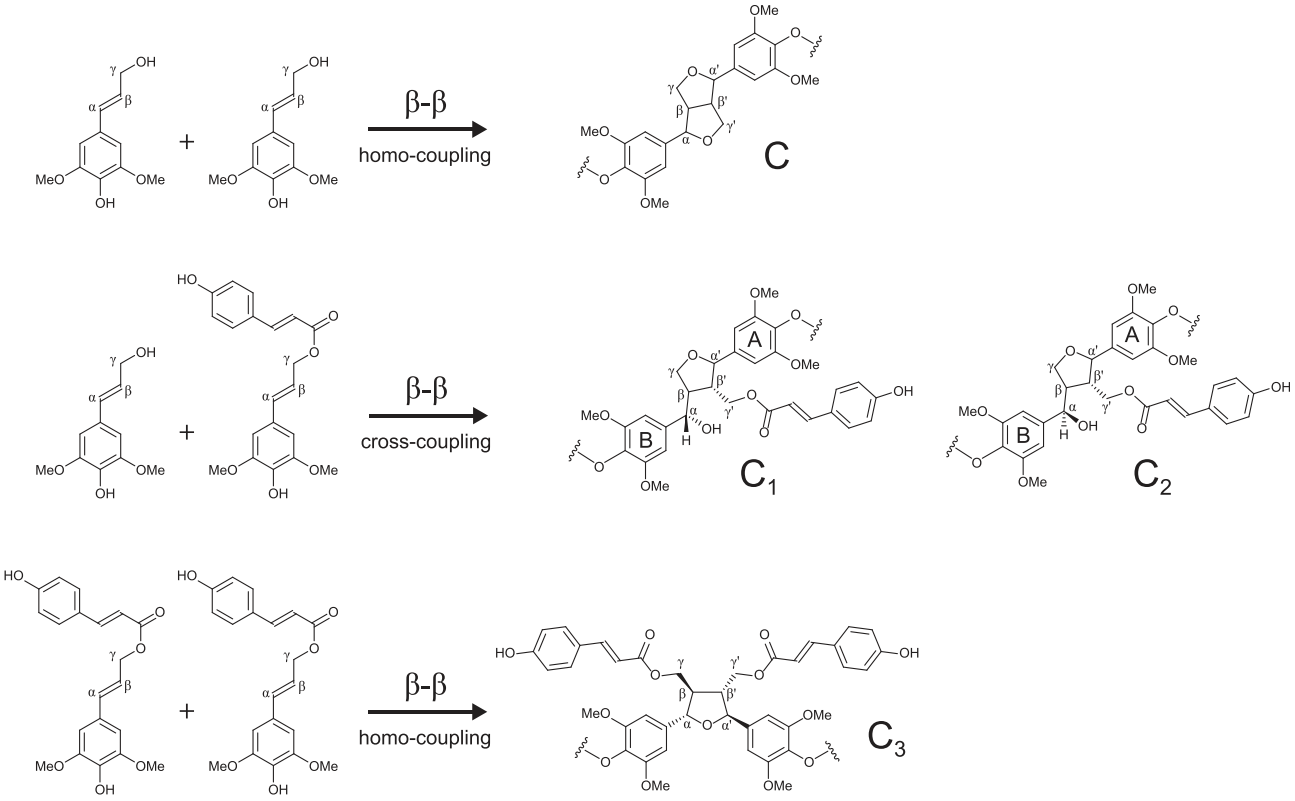

Fig. 8. Resinol **C** and tetrahydrofurans produced from β–β′-homo-dimerization of sinapyl *p*-coumarate (**C3**) and its cross-coupling with sinapyl alcohol (**C1**, **C2**). (Adapted from Refs. [47,59]).

γ-OH, as seen by HMBC. Similar results were also observed in the lignin from wheat straw [28], where only traces of γ-*p*-coumaroylated syringyl conjugates were released, despite the occurrence of significant amounts of *p*-coumarates being attached to the γ-OH. This finding seems to indicate that, as also occurred in the lignin from wheat straw, *p*-coumarate groups mostly acylate the γ-OH in condensed lignin substructures that are not amenable to DFRC analysis, a slightly troubling observation that requires further study. This is however supported by the below-noted observation of the products of sinapyl *p*-coumarate homodimerization units **C3**. The assumption is also supported by the presence of an intense signal for γ-acylated β–*O*–4′ substructures linked to G-units in the HSQC spectrum of the MWL from sugarcane straw (Fig. 4B) that indicates a significant γ-acylation of G-units in this lignin, and which is absent in the spectrum of the MWL from sugarcane bagasse (Fig. 3B). The DFRC′ data also revealed a minor extent of γ-acylation of these lignins with acetate groups, but which takes place predominantly on G units (3.7% and 3.3% of G-lignin units were acetylated in the lignins from bagasse and straw, respectively) rather than on S units (only 0.8% and 1.8%). Low levels of lignin acetylation, with a preference for G-units, have also been found in other grasses, such as bamboo, wheat straw, or the pith of elephant grass [24,28,36]. In contrast, in the lignin of most plants, γ-acetylation occurs predominantly on S-units [31,36,58]. This fact seems to indicate that as yet unknown acetyl transferases with a higher affinity towards coniferyl alcohol than towards sinapyl alcohol, contrary to what occurs in most plants, are probably involved in monolignol acetylation in grasses.

3.5. Diversity of β–β (resinol and tetrahydrofuran) structures in the lignins from sugarcane bagasse and straw

The HSQC spectra of the lignins from sugarcane bagasse and straw clearly show the presence of significant amounts of a tetrahydrofuran structure (**C3**) arising from β–β coupling of two γ-acylated monolignols. As *p*-coumarates are the main group acylating the lignin, and predominantly on S-units, it is evident that the tetrahydrofuran structure **C3** identified in the HSQC spectra has been produced from the β–β′-coupling of two sinapyl *p*-coumarate monomers, as shown in Fig. 8. These units have been found in the lignins from other grasses, such as maize and elephant grass [24,47], and analogous structures bearing acetates or *p*-hydroxybenzoates have also been identified in the lignins from other plants [47,55,56,59].

Besides tetrahydrofuran structure **C3**, the β–β coupling and cross-coupling of sinapyl alcohol and γ-*p*-coumaroylated sinapyl alcohol can form non-symmetrical tetrahydrofurans **C1** and **C2**, as detailed in Fig. 8. A wide variety of tetrahydrofuran structures arising from β–β coupling and cross-coupling of normal γ-OH and γ-acylated (with acetates, *p*-coumarates and *p*-hydroxybenzoates) monolignols, have been synthesized in past years and their different correlation signals assigned in the HSQC spectra [47,55,56,59]. In those papers, the different synthetic structures were acetylated to improve the spectral properties. Therefore, in order to have detailed information of the different β–β resinol and tetrahydrofuran structures present in the lignins here, the MWLs were acetylated and the HSQC correlation signals were compared with those previously published [47,55,56,59]. Fig. 9 shows the 2D-NMR HSQC spectra of the (acetylated) MWLs from sugarcane bagasse and straw, with the C_α/H_α and C_β/H_β and C_γ/H_γ correlations of the different resinol and tetrahydrofuran structures arising from the β–β coupling and cross-coupling of sinapyl alcohol and sinapyl *p*-coumarate. The signals observed closely match those previously reported for synthesized model compounds and related lignins and provide compelling evidence for the occurrence of the various tetrahydrofuran structures arising from the β–β homo-coupling of

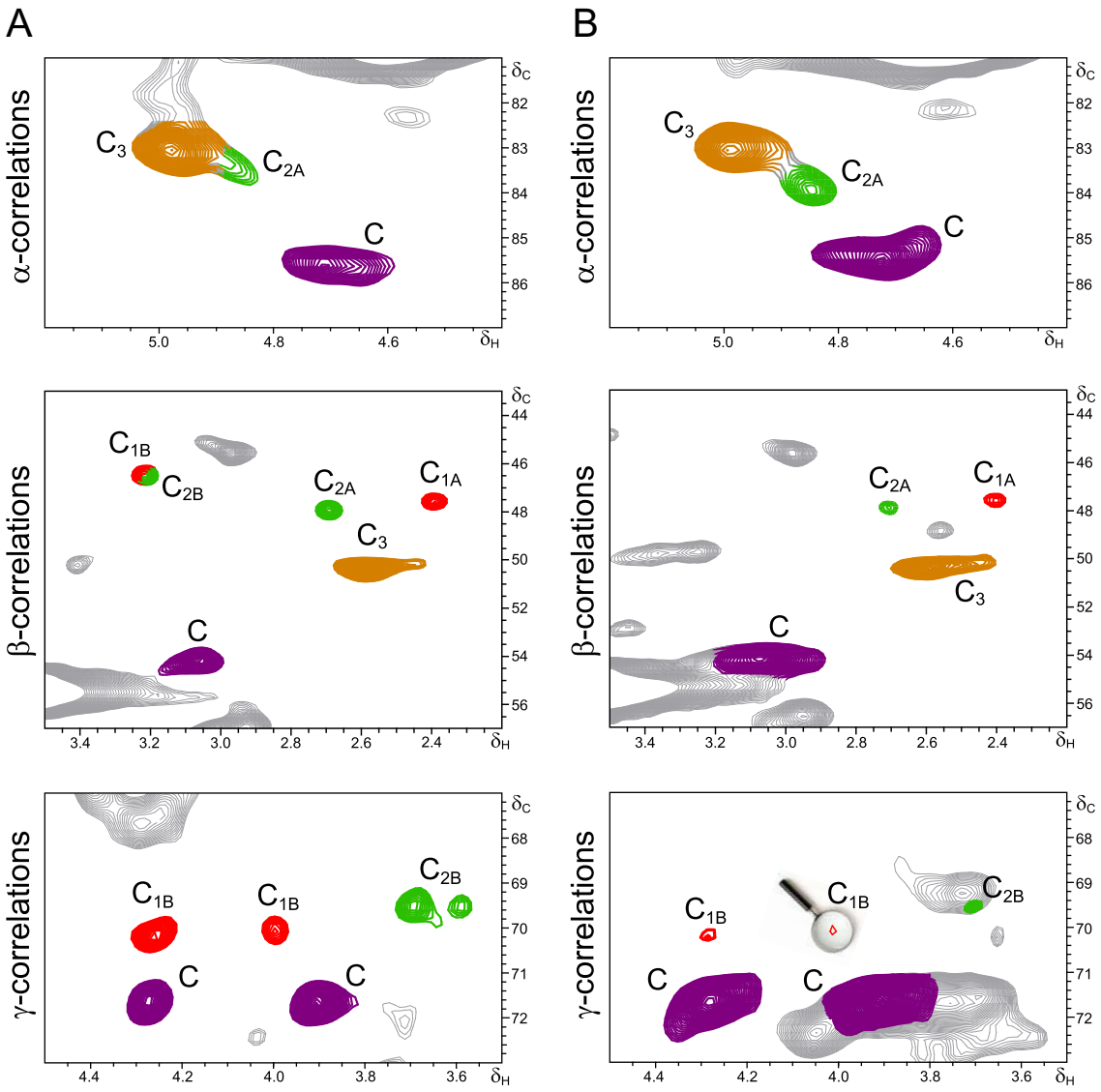

Fig. 9. 2D-NMR HSQC of the (acetylated) MWLs from (**A**) sugarcane bagasse and (**B**) straw showing the C_α/H_α and C_β/H_β and C_γ/H_γ correlations of the different β–β resinol **C** and tetrahydrofuran $\mathbf{C_1}$–$\mathbf{C_3}$ structures arising from the coupling and cross-coupling of sinapyl alcohol and sinapyl *p*-coumarate, as depicted in Fig. 8. Signals were assigned from previously published literature [47,59].

sinapyl *p*-coumarate ($\mathbf{C_3}$) as well as its cross-coupling with sinapyl alcohol ($\mathbf{C_1}$ and $\mathbf{C_2}$), together with the presence of traditional β–β resinol structures (**C**). The occurrence of the tetrahydrofuran structures $\mathbf{C_1}$–$\mathbf{C_3}$ in these lignins conclusively demonstrates that the sinapyl *p*-coumarate conjugate acts as a monomer participating in coupling and cross-coupling reactions during lignification of sugarcane, and therefore implicates the presence of corresponding *p*-coumaroyl-CoA:monolignol transferases (PMTs) in this plant. In fact, the *PMTs* involved in the *p*-coumaroylation of monolignols have been discovered in corn [43], and in the model grass *Brachypodium distachyon* [60] in which a candidate gene has been recently identified and its action validated [61].

4. Conclusions

This paper describes the differences in composition and structure of the lignins from sugarcane bagasse and straw, the two major residues produced from the sugarcane industry. Whereas the lignin from sugarcane bagasse is S-rich (H:G:S molar ratio of 2:38:60), the lignin from sugarcane straw is G-rich (4:68:28). The compositional differences are also reflected in differences in the relative abundances of the various interunit linkages in both lignins. Thus, the lignin from bagasse is mostly made up by alkyl-aryl ether substructures (β–*O*–4′, accounting for 83% of all the measured interunit linkage types), followed by minor amounts of phenylcoumarans (β–5′, 6%) and other condensed linkages. The lignin from straw, on the other hand, has lower amounts of alkyl-aryl ether substructures (75% of all interunit linkages) and has higher amounts of condensed structures such as phenylcoumarans (15%) and dibenzodioxocins (5–5′/4–O–β′, 3%), as is consistent with a lignin enriched in G-units. The degree of lignin acylation by *p*-coumarate and acetate also differs strikingly, being higher in the bagasse. The structural differences observed in the lignins of the two sugarcane residues, bagasse from the stems after expelling the sugar, and straw from the residual plant (including leaves), indicates that the pretreatment methods needed to reduce the recalcitrance of the cell wall will have to be optimized for each residue. In particular, the structures of the lignins in both resides suggest that the bagasse material will pretreat more easily (because of its higher syringyl content and lower condensation degree) than

the straw (with a higher content of condensed structures). In addition, the two residues contain, as well as the polysaccharides that may be saccharified and fermented to liquid biofuels and lignins that might be valorized, significant levels of *p*-coumarate, ferulate, and tricin that might be valuable to extract as commodity chemicals. Optimizing the utilization of all of the plant biomass that is sustainably available will improve biorefinery operations and help to offer fuels and chemicals with a reduced carbon footprint compared to fossil-derived products.

Acknowledgments

This study has been funded by the Spanish projects AGL2011-25379, AGL2014-53730-R and CTQ2014-60764-JIN (co-financed by FEDER funds), the CSIC project 2014-40E-097 and the EU-projects LIGNODECO (KBBE-2009-3-244362) and INDOX (KBBE-2013-7-613549). John Ralph was funded through the DOE Great Lakes Bioenergy Research Center (Department of Energy's Biological and Environmental Research Office of Science DE-FC02-07ER64494). Jorge Rencoret thanks the CSIC for a JAE-DOC contract of the program “Junta para la Ampliación de Estudios” co-financed by Fondo Social Europeo (FSE). A.G. Lino thanks CAPES (Coordenação de Aperfeiçoamento de Pessoal de Nível Superior) for financial support. C.F. Lima and J.L. Colodette are grateful to National Council for Scientific and Technological Development (CNPq) for research fellowships. We also thank Dr. Manuel Angulo for performing the NMR analyses that were acquired on a Bruker Avance III 500 MHz instrument from the NMR facilities of the General Research Services of the University of Seville (SGI-CITIUS).

References

[1] F. Santos, A. Borém, C. Caldas, Sugarcane: Bioenergy, Sugar and Ethanol – Technology and Prospects, Universidade Federal de Viçosa, Viçosa, Brazil, 2012.
[2] A.P. de Souza, A. Grandis, D.C.C. Leite, M.S. Buckeridge, Sugarcane as a bioenergy source: history, performance and perspectives for second generation bioethanol, Bioenergy Res. 7 (2014 Aug) 24–35.
[3] FAOSTAT [database on the Internet]. Rome – Italy: Food and Agriculture Organization of the United Nations; 2015-[cited 2015 Jun 10] Production, Crops, Sugar Cane; Available from: http://faostat3.fao.org Files updated Annually.
[4] P.S. Ortiz, S. de Oliveira, Exergy analysis of pretreatment processes of bioethanol production based on sugarcane bagasse, Energy 76 (2014 Nov) 130–138.
[5] A.J. Ragauskas, C.K. Williams, B.H. Davison, G. Britovsek, J. Cairney, C.A. Eckert, et al., The path forward for biofuels and biomaterials, Science 311 (5760) (2006) 484–489.
[6] M.F. Andrade, J.L. Colodette, Dissolving pulp production from sugar cane bagasse, Ind. Crops Prod. 52 (2014 Jan) 58–64.
[7] C.A. Cardona, J.A. Quintero, I.C. Paz, Production of bioethanol from sugarcane bagasse: status and perspectives, Bioresour. Technol. 101 (13) (2010) 4754–4766.
[8] S.C. Rabelo, A.C. da Costa, Vaz Rossel CE. Industrial waste recovery, in: F. Santos, A. Borém, C. Caldas (Eds.), Sugarcane: Bioenergy, Sugar and Ethanol – Technology and Prospects, Universidade Federal de Viçosa, Viçosa, Brazil, 2012, pp. 449–470.
[9] L.R.M. Oliveira, V.M. Nascimento, A.R. Gonçalves, G.J.M. Rocha, Combined process system for the production of bioethanol from sugarcane straw, Ind. Crops Prod. 58 (2014 Jul) 1–7.
[10] G.J.M. Rocha, A.R. Gonçalves, B.R. Oliveira, E.G. Olivares, C.E.V. Rossell, Steam explosion pretreatment reproduction and alkaline delignification reactions performed on a pilot scale with sugarcane bagasse for bioethanol production, Ind. Crops Prod. 35 (1) (2012) 274–279.
[11] G.J.M. Rocha, V.M. Nascimento, V.F.N. da Silva, D.L.S. Corso, A.R. Gonçalves, Contributing to the environmental sustainability of the second generation ethanol production: delignification of sugarcane bagasse with sodium hydroxide recycling, Ind. Crops Prod. 59 (2014 Aug) 63–68.
[12] H. Mou, E. Heikkilä, P. Fardim, Topochemistry of environmentally friendly pretreatments to enhance enzymatic hydrolysis of sugar cane bagasse to fermentable sugars, J. Agric. Food Chem. 62 (16) (2014) 3619–3625.
[13] L.A.R. Batalha, Q. Han, H. Jameel, H.-M. Chang, J.L. Colodette, F.J.B. Gomes, Production of fermentable sugars from sugarcane bagasse by enzymatic hydrolysis after autohydrolysis and mechanical refining, Bioresour. Technol. 180 (2015 Mar) 97–105.
[14] J. Ralph, K. Lundquist, G. Brunow, F. Lu, H. Kim, P.F. Schatz, et al., Lignins: Natural polymers from oxidative coupling of 4-hydroxyphenylpropanoids, Phytochem. Rev. 3 (1–2) (2004) 29–60.
[15] J. Ralph, Hydroxycinnamates in lignification, Phytochem. Rev. 9 (1) (2010) 65–83.
[16] J.-X. Sun, X.-F. Sun, R.-C. Sun, P. Fowler, M.S. Baird, Inhomogeneities in the chemical structure of sugarcane bagasse lignin, J. Agric. Food Chem. 51 (23) (2003) 6719–6725.
[17] A.-P. Zhang, C.-F. Liu, R.-C. Sun, J. Xie, Extraction, purification, and characterization of lignin fractions from sugarcane bagasse, BioResources 8 (2) (2013) 1604–1614.
[18] J. Zeng, Z. Tong, L. Wang, J.Y. Zhu, L. Ingram, Isolation and structural characterization of sugarcane bagasse lignin after dilute phosphoric acid plus steam explosion pretreatment and its effect on cellulose hydrolysis, Bioresour. Technol. 154 (2014 Feb) 274–281.
[19] A. Bottcher, I. Cesarino, A.B. dos Santos, R. Vicentini, J.L.S. Mayer, R. Vanholme, et al., Lignification in sugarcane: biochemical characterization, gene discovery, and expression analysis in two genotypes contrasting for lignin content, Plant Physiol. 163 (4) (2013) 1539–1557.
[20] Tappi Standard Test Methods 2004-2005, Tappi Test Methods, Tappi Press, Atlanta, GA, 2004.
[21] A. Darwill, M. McNeil, P. Albersheim, D. Delmer, The primary cell-walls of flowering plants, in: N. Tolbert (Ed.), The Biochemistry of Plants, Academic Press, New York, 1980, pp. 91–162.
[22] B.L. Browning, Methods of Wood Chemistry, vol. II, Wiley-Interscience Publishers, New York, 1967.
[23] A. Björkman, Studies on finely divided wood. Part I. Extraction of lignin with neutral solvents, Sven. Papperstidn 59 (13) (1956) 477–485.
[24] J.C. del Río, P. Prinsen, J. Rencoret, L. Nieto, J. Jiménez-Barbero, J. Ralph, et al., Structural characterization of the lignin in the cortex and pith of elephant grass (*Pennisetum purpureum*) stems, J. Agric. Food Chem. 60 (14) (2012) 3619–3634.
[25] J. Ralph, R.D. Hatfield, Pyrolysis-GC/MS characterization of forage materials, J. Agric. Food Chem. 39 (8) (1991) 1426–1437.
[26] H. Kim, J. Ralph, T. Akiyama, Solution-state 2D NMR of ball-milled plant cell-wall gels in DMSO-d_6, Bioenergy Res. 1 (1) (2008) 56–66.
[27] J. Rencoret, G. Marques, A. Gutiérrez, L. Nieto, J.I. Santos, J. Jiménez-Barbero, et al., HSQC-NMR analysis of lignin in woody (*Eucalyptus globulus* and *Picea abies*) and non-woody (*Agave sisalana*) ball-milled plant materials at the gel state, Holzforschung 63 (6) (2009) 691–698.
[28] J.C. del Río, J. Rencoret, P. Prinsen, Á.T. Martínez, J. Ralph, A. Gutiérrez, Structural characterization of wheat straw lignin as revealed by analytical pyrolysis, 2D-NMR, and reductive cleavage methods, J. Agric. Food Chem. 60 (23) (2012) 5922–5935.
[29] S.A. Ralph, J. Ralph, L. Landucci, NMR Database of Lignin and Cell Wall Model Compounds, 2009. https://www.glbrc.org/databases_and_software/nmrdatabase/ (accessed: January 2009).
[30] J. Ralph, L.L. Landucci, NMR of lignins, in: C. Heitner, D.R. Dimmel, J.A. Schmidt (Eds.), Lignin and Lignans – Advances in Chemistry, CRC Press, Boca Raton, FL, 2010, pp. 137–234.
[31] J.C. del Río, J. Rencoret, G. Marques, A. Gutiérrez, D. Ibarra, J.I. Santos, et al., Highly acylated (acetylated and/or *p*-coumaroylated) native lignins from diverse herbaceous plants, J. Agric. Food Chem. 56 (20) (2008) 9525–9534.
[32] F. Lu, J. Ralph, Derivatization followed by reductive cleavage (DFRC method), a new method for lignin analysis: protocol for analysis of DFRC monomers, J. Agric. Food Chem. 45 (7) (1997) 2590–2592.
[33] F. Lu, J. Ralph, The DFRC method for lignin analysis. Part 1. A new method for β-aryl ether cleavage: lignin model studies, J. Agric. Food Chem. 45 (12) (1997) 4655–4660.
[34] F. Lu, J. Ralph, Detection and determination of *p*-coumaroylated units in lignins, J. Agr Food Chem. 47 (5) (1999) 1988–1992.
[35] J. Ralph, F. Lu, The DFRC method for lignin analysis. 6. A simple modification for identifying natural acetates in lignin, J. Agric. Food Chem. 46 (11) (1998) 4616–4619.
[36] J.C. del Río, G. Marques, J. Rencoret, A.T. Martínez, A. Gutiérrez, Occurrence of naturally acetylated lignin units, J. Agric. Food Chem. 55 (14) (2007) 5461–5468.
[37] G.J.M. Rocha, V.M. Nascimento, A.R. Gonçalves, V.F.N. Silva, C. Martín, Influence of mixed sugarcane bagasse samples evaluated by elemental analysis and physical-chemical composition, Ind. Crops Prod. 64 (2015 Feb) 52–58.
[38] J.C. del Río, A. Gutiérrez, I.M. Rodríguez, D. Ibarra, A.T. Martínez, Composition of non-woody plant lignins and cinnamic acids by Py-GC/MS, Py/TMAH and FT-IR, J. Anal. Appl. Pyrol 79 (1–2) (2007) 39–46.
[39] J. Rencoret, P. Prinsen, A. Gutiérrez, A.T. Martínez, J.C. del Río, Isolation and structural characterization of the milled wood lignin, dioxane lignin, and cellulolytic lignin preparations from brewer's spent grain, J. Agric. Food Chem. 63 (2) (2015) 603–613.
[40] J.H. Grabber, S. Quideau, J. Ralph, *p*-Coumaroylated syringyl units in maize lignin: Implications for β-ether cleavage by thioacidolysis, Phytochemistry 43 (6) (1996) 1189–1194.
[41] J.H. Grabber, J. Ralph, R.D. Hatfield, Cross-linking of maize walls by ferulate dimerization and incorporation into lignin, J. Agr Food Chem. 48 (12) (2000) 6106–6113.
[42] J.H. Grabber, F. Lu, Formation of syringyl-rich lignins in maize as influenced by feruloylated xylans and *p*-coumaroylated monolignols, Planta 226 (3) (2007) 741–751.

[43] R.D. Hatfield, J.M. Marita, K. Frost, J. Grabber, J. Ralph, F. Lu, et al., Grass lignin acylation: *p*-coumaroyl transferase activity and cell wall characteristics of C3 and C4 grasses, Planta 229 (6) (2009) 1253–1267.
[44] J.C. del Río, F. Martín, F.J. González-Vila, Thermally assisted hydrolysis and alkylation as a novel pyrolytic approach for the structural characterization of natural biopolymers and geomacromolecules, Trends Anal. Chem. 15 (2) (1996) 70–79.
[45] F. Martín, J.C. del Río, F.J. González-Vila, T. Verdejo, Thermally assisted hydrolysis and alkylation of lignins in the presence of tetra-alkylammonium hydroxides, J. Anal. Appl. Pyrol 35 (1) (1995) 1–13.
[46] J. Ralph, R.D. Hatfield, S. Quideau, R.F. Helm, J.H. Grabber, H.-J.G. Jung, Pathway of *p*-coumaric acid incorporation into maize lignin as revealed by NMR, J. Am. Chem. Soc. 116 (21) (1994) 9448–9456.
[47] F. Lu, J. Ralph, Novel β–β structures in lignins incorporating acylated monolignols, Appita (2005 May) 233–237.
[48] J.-L. Wen, S.-L. Su, B.-L. Xue, R.-C. Sun, Quantitative structural characterization of the lignins from the stem and pith of bamboo (*Phyllostachys pubescens*), Holzforschung 67 (6) (2013) 613–627.
[49] T.-T. You, J.-Z. Mao, T.-Q. Yuan, J.-L. Wen, F. Xu, Structural elucidation of the lignins from stems and foliage of *Arundo donax* Linn, J. Agric. Food Chem. 61 (22) (2013) 5361–5370.
[50] W. Lan, F. Lu, M. Regner, Y. Zhu, J. Rencoret, S.A. Ralph, et al., Tricin, a flavonoid monomer in monocot lignification, Plant Phys. 167 (4) (2015) 1284–1295.
[51] J. Rencoret, J. Ralph, G. Marques, A. Gutiérrez, A.T. Martínez, J.C. del Río, Structural characterization of lignin isolated from coconut (*Cocos nucifera*) coir fibers, J. Agric. Food Chem. 61 (10) (2013) 2434–2445.
[52] L.L. Landucci, G.C. Deka, D.N. Roy, A ^{13}C NMR study of milled wood lignins from hybrid Salix clones, Holzforschung 46 (6) (1992) 505–511.
[53] R.C. Sun, J.M. Fang, J. Tomkinson, Fractional isolation and structural characterization of lignins from oil palm trunk and empty fruit bunch fibres, J. Wood Chem. Technol. 19 (1–2) (1999) 335–356.
[54] K. Kuroda, T. Ozawa, T. Ueno, Characterization of sago palm (*Metroxylon sagu* Rottb.) lignin by analytical pyrolysis, J. Agric. Food Chem. 49 (4) (2001) 1840–1847.
[55] F. Lu, J. Ralph, K. Morreel, E. Messens, W. Boerjan, Preparation and relevance of a cross-coupling product between sinapyl alcohol and sinapyl *p*-hydroxybenzoate, Org. Biomol. Chem. 2 (20) (2004) 2888–2890.
[56] F. Lu, S.D. Karlen, M. Regner, H. Kim, S.A. Ralph, R.-C. Sun, et al., Naturally *p*-hydroxybenzoylated lignins in palms, Bioenergy Res. (2015), http://dx.doi.org/10.1007/s12155-015-9583-4 in press).
[57] F. Lu, J. Ralph, Preliminary evidence for sinapyl acetate as a lignin monomer in kenaf, Chem. Commun. 1 (2002 Jan) 90–91.
[58] J. Ralph, An unusual lignin from kenaf, J. Nat. Prod. 59 (4) (1996) 341–342.
[59] F. Lu, J. Ralph, Novel tetrahydrofuran structures derived from β–β-coupling reactions involving sinapyl acetates in kenaf lignins, Org. Biomol. Chem. 6 (20) (2008) 3681–3694.
[60] S. Withers, F. Lu, H. Kim, Y. Zhu, J. Ralph, C.G. Wilkerson, Identification of a grass-specific enzyme that acylates monolignols with *p*-coumarate, J. Biol. Chem. 287 (11) (2012) 8347–8355.
[61] D. Petrik, S.D. Karlen, C. Cass, D. Padmakshan, F. Lu, S. Liu, et al., *p*-Coumaroyl-CoA:monolignol transferase (PMT) acts specifically in the lignin biosynthetic pathway in *Brachypodium distachyon*, Plant J. 77 (5) (2014) 713–726.